Multiple Forces Contribute to Cell Sheet Morphogenesis for Dorsal Closure in *Drosophila*

Daniel P. Kiehart, Catherine G. Galbraith, Kevin A. Edwards, Wayne L. Rickoll, and Ruth A. Montague

Department of Cell Biology, Cell and Molecular Biology Program, University Program in Genetics and the Duke Comprehensive Cancer Center, Duke University Medical Center, Durham, North Carolina 27710-3709

Abstract. The molecular and cellular bases of cell shape change and movement during morphogenesis and wound healing are of intense interest and are only beginning to be understood. Here, we investigate the forces responsible for morphogenesis during dorsal closure with three approaches. First, we use real-time and time-lapsed laser confocal microscopy to follow actin dynamics and document cell shape changes and tissue movements in living, unperturbed embryos. We label cells with a ubiquitously expressed transgene that encodes GFP fused to an autonomously folding actin binding fragment from fly moesin. Second, we use a biomechanical approach to examine the distribution of stiffness/tension during dorsal closure by following the response of the various tissues to cutting by an ultraviolet laser. We tested our previous model (Young, P.E., A.M. Richman, A.S. Ketchum, and D.P. Kiehart. 1993. *Genes Dev.* 7:29–41) that the leading edge of the lateral epidermis is a contractile purse-string that provides force for dorsal closure. We show that this structure is under tension and behaves as a supracellular purse-string, however, we provide evidence that it alone cannot account for the forces responsible for dorsal closure. In addition, we show that there is isotropic stiffness/tension in the amnioserosa and anisotropic stiffness/tension in the lateral epidermis. Tension in the amnioserosa may contribute force for dorsal closure, but tension in the lateral epidermis opposes it. Third, we examine the role of various tissues in dorsal closure by repeated ablation of cells in the amnioserosa and the leading edge of the lateral epidermis. Our data provide strong evidence that both tissues appear to contribute to normal dorsal closure in living embryos, but surprisingly, neither is absolutely required for dorsal closure. Finally, we establish that the *Drosophila* epidermis rapidly and reproducibly heals from both mechanical and ultraviolet laser wounds, even those delivered repeatedly. During healing, actin is rapidly recruited to the margins of the wound and a newly formed, supracellular purse-string contracts during wound healing. This result establishes the *Drosophila* embryo as an excellent system for the investigation of wound healing. Moreover, our observations demonstrate that wound healing in this insect epidermal system parallel wound healing in vertebrate tissues in situ and vertebrate cells in culture (for review see Kiehart, D.P. 1999. *Curr. Biol.* 9:R602–R605).

Key words: wound healing • actin • biomechanical • amnioserosa • GFP moesin

Introduction

Morphogenesis is the complex set of processes by which the mature forms of a cell, tissue, organ or organism develop. It is the end result of processes that begin with pattern formation and cellular proliferation, and continues through determination and differentiation. Throughout these processes, cell movements, rearrangements, and shape changes contribute to the final form that defines the tissues, organ, or organism.

Cellular movements and rearrangements are diverse and complex, and are recapitulated throughout phylogeny. For example, ventral furrow formation and posterior midgut invagination, which are elements of early gastrulation in *Drosophila*, are both characterized by cell shape changes, placode formation, apical wedging, and cell sheet morphogenesis. These morphogenic processes are very similar to the cell movements that characterize neurulation in vertebrates (Young et al., 1991; Smith and Schoenwolf, 1997; Leptin, 1999). Comparably, dorsal closure in *Drosophila* (Young et al., 1993; Knust, 1997; Agnes and Noselli, 1999) involves cell sheet spreading, which mimics ventral enclosure in *Caenorhabditis elegans* (Williams-

The online version of this article contains supplemental material.

Address correspondence to Daniel P. Kiehart, Box 3079, Department of Cell Biology, 307B Nanaline Duke Building, Duke University Medical Center, Durham NC 27710-3709. Tel.: (919) 681-8079. Fax: (919) 684-5481. E-mail: d.kiehart@cellbio.duke.edu

Masson et al., 1997), aspects of cell sheet spreading during epiboly (Keller, 1980; Keller and Trinkaus, 1987), and wound healing in certain epithelia (Martin and Lewis, 1992; Bement et al., 1993, 1999; Martin, 1997; Kiehart, 1999).

The molecular basis of development, from pattern formation to cell shape change, has been under intense scrutiny. Wide-ranging studies in phylogenetically diverse organisms have contributed greatly to our understanding of the gene products that are required for pattern formation, signal transduction, and determination. In contrast, our understanding of the cellular and molecular basis of morphogenesis is considerably limited. For example, studies on cell rearrangements show that both germ band extension in *Drosophila* (Irvine and Wieschaus, 1994) and gastrulation in *Xenopus* (Elul et al., 1997) are due to a process termed convergent extension, whereby adjacent cells intercalate to transform a short, wide tissue into a long, narrow one. The molecular mechanism of these convergent extensions is not understood. Convergent extensions are likely to require alterations in cell–cell adhesion, cell interactions with the extracellular matrix, and changes in the organization of the dynamic cytoskeleton and the function of chemomechanical force producers (so-called motor proteins) that produce force for cell shape change and locomotion. Indeed, a complete understanding of morphogenesis will require a description of the motor proteins, the molecular switches that regulate motor protein function, and the molecular linkers that integrate motor protein function to coordinate the cell shape changes, rearrangements, and movements that the motor proteins drive.

Ultimately, a key part of understanding how an ensemble of proteins collaborates to produce force is understanding the distribution of the forces themselves. We became interested in morphogenesis during the dorsal closure stages of the *Drosophila* embryo when we found that defects in the nonmuscle myosin heavy chain caused a failure of dorsal closure (Young et al., 1993; see Fig. 1 here and in Young et al., 1993 for an understanding of the movements of dorsal closure; for review see Knust, 1997; Agnes and Noselli, 1999). We mapped changes in cell shape at the surface of the embryo by examining fixed embryos that were stained with anti–α-spectrin antibody, a reagent that outlines cell shape because of the cortical distribution of the spectrin. We found that elongation of epidermal cells perpendicular to the long axis of the embryo could explain the change in surface area required to cover the amnioserosa (Young et al., 1993). Further, we found that nonmuscle myosin II is localized to the leading edge of the cells of the lateral epidermis and, therefore, might power the advance of the lateral epidermis up and over the underlying amnioserosa during dorsal closure.

Our observations on myosin localization and function led us to propose a simple model for how forces for dorsal closure might be produced. We proposed that myosin and actin form a mechanically contiguous contractile band, or supracellular purse-string, composed of a series of intracellular contractile bars (positioned at the leading edge of the lateral epidermis), whose integrity requires strong intercellular connections. Further, we proposed that the contraction of this purse-string alone might be sufficient to power the cell movements during dorsal closure. Subsequent studies have confirmed our observations on shape changes in the lateral epidermis, and have gone on to investigate the pathways that are required for these morphological changes. Such studies have shown that some essential components of the signaling pathway include the small GTP binding proteins in the Rho, Rac, Cdc42 subfamily, the JUN kinase cascade, and the TGFβ homologue, *decapentaplegic* (Agnes and Noselli, 1999; Harden et al., 1999; Li et al., 1999; Liu et al., 1999; Lu and Settleman, 1999; Ricos et al., 1999; Sawamoto et al., 1999; Zecchini et al., 1999).

Here, we investigate dorsal closure in three ways. First, we use real-time and time-lapsed laser confocal microscopy to follow cell shape changes and tissue movements in living, experimentally unperturbed *Drosophila* embryos that express a green fluorescent fusion protein. This GFP fusion protein binds to actin and outlines cell shape. Second, we present experiments designed to investigate the forces that contribute to morphogenesis during dorsal closure using a biomechanical approach. As cells grow and change morphology, an intrinsic or resting tension develops within tissues and organs. Such tensions are a manifestation of the forces that contribute to tissue movements and rearrangements over developmental time. Our analysis of the distribution of forces in the embryonic ectoderm suggests that purse-string forces in the leading edge of the lateral epidermis and cell autonomous contractility in the amnioserosa both contribute to cell movements during dorsal closure. In contrast, tension in the anisotropic lateral epidermis produces forces that oppose dorsal closure. Together, our observations put key constraints on models that explain dorsal closure.

Third, we investigate whether particular regions of the embryo are essential for dorsal closure by using a laser-induced wound to repeatedly compromise their mechanical integrity. We provide strong evidence that the integrity of neither the supracellular purse-string nor the amnioserosa is strictly required for dorsal closure. However, repeated ablation of both the leading edge of the lateral epidermis and the amnioserosa block dorsal closure. Interpretation of these experiments is not straightforward because repeated, double ablations result in severe damage to the embryo. Overall, we conclude that in wild-type embryos, multiple forces contribute to dorsal closure.

Finally, we establish that the *Drosophila* epidermis rapidly and reproducibly heals from both mechanical and ultraviolet laser wounds, even those delivered repeatedly. Early in the process, actin is recruited to the margins of the wound and contraction of a supracellular purse-string accompanies wound healing. These observations establish the *Drosophila* embryo as an excellent system for investigation of the cellular and molecular basis of wound healing.

Materials and Methods

sGMCA Provides a Reagent to Follow Shape Change during Morphogenesis In Vivo

Based on our success using a green fluorescent protein (GFP)[1] fused to an

[1]*Abbreviation used in this paper:* GFP, green fluorescent protein.

actin binding protein, we constructed a second generation fusion protein. It consists of humanized (for codon bias) GFP containing the S65T mutation (CLONTECH Laboratories), which speeds protein folding and increases the quantum efficiency of the GFP, fused to the same fragment of moesin that includes the extended helical region and the actin binding sequences (Edwards et al., 1997). Our original construct (called hsGFPmoe) used a heat shock driven promoter because we feared that constitutive expression of the moesin fusion construct might have deleterious effects on fly development. Based on our observations that flies harboring the hsGFPmoe transgene could be heat-shocked daily and still survive as a viable stock, we used a promoter/enhancer construct from the ubiquitously expressed *spaghetti squash* gene, which encodes the single, nonmuscle myosin II regulatory light chain (Karess et al., 1991; Wheatley et al., 1995; Edwards and Kiehart, 1996; Jordan and Karess, 1997). This construct, called sGMCA, was used to establish stable transgenic fly lines through P element–based germ line transformation. The construct appears to be expressed ubiquitously and does not appear to be deleterious to any aspect of fly development or behavior, although the stocks are not as robust as our healthiest stocks (e.g., wild-type Oregon R or w^{1118}). The line that we use most is called sGMCA-3.1 and has the transgene construct inserted on the third chromosome, but other insertions behave in an indistinguishable fashion. Fly stocks can be established in which the sGMCA-3.1 chromosome is homozygous, demonstrating that the transgenic construct is inserted in a nonessential part of the genome. The complete sequence of sGMCA in its P element vector is provided as Supplemental Figure 1 (sGMCA sequence and annotation), which is available at http://www.jcb.org/cgi/content/full/149/2/471/DC1.

Embryo Handling and Microscopy

sGMCA flies were grown using standard methods in small population cages on grape agar plates and yeast paste (Wieschaus and Nusslein-Volhard, 1986). Embryos were aligned on an agar pad, picked up on an embryo glue–coated coverslip, and mounted on a micromanipulation chamber or a modified, Teflon window chamber that provided a gas permeable membrane, which allowed development to proceed (Kiehart et al., 1994). All images were obtained with a Bio-Rad 600, scanning laser confocal microscope mounted on a Zeiss Axioscope microscope. Zeiss objectives included 40× 0.9 NA, 25× 0.8 NA, and 16× 0.5 NA multiimmersion, infinity-corrected objectives. Microbeam irradiations (see below) were all done through the 40× lens.

Mechanical Disruption of Embryonic Tissues

Mechanical wounds were made with a fine glass pipette with a tip diameter of <0.5 μm. To image the pipette with the confocal system, we filled it with fluorescein dextran. The embryo was mounted dorsal side up in a standard micromanipulation chamber. We inserted the pipette into the flank of the embryo, just below the leading edge of the lateral epidermis. The pipette was adjusted to have a slight, upward incline. With the pipette tip centered in the embryo, we raised it through the yolk until it pushed the amnioserosa and the vitelline membrane against the coverslip and began to flex. To cut the leading edge, we drew the pipette out of the embryo while it remained pressed against the coverslip.

Laser Ablation of Embryonic Tissues

To optically cut embryonic tissue, we used an ultraviolet laser as follows. An N_2 laser (model VSL-337ND; Laser Science, Inc.) that produces 3-ns pulses of 6 μJ (at the source) of 337.1 nm UV light was mounted on the microscope table. Surface mirrors were used to direct the laser through a small, adjustable diaphragm, into the epiilluminator port of a Zeiss Axioscope microscope. Standard epiilluminator components (lamp house, epicollector, and diaphragm) were removed to avoid absorption by glass elements. Thus, the first optical component in the microscope that the laser light hit was a UV reflecting, dichroic mirror (model 400DCLP; Chroma Technology Corp.) mounted in the Zeiss filter set slider (both the exciter filter and the barrier filter were removed from that slider position). The beam was thereby directed down through the objective and onto the specimen. The dose of UV light delivered was adjusted by counting the number of pulses at 1–3 Hz. An audible click emitted by the laser at each pulse facilitated the counting process. The objective focused the parallel rays of the UV, laser light onto the specimen. The intensity of the laser light at the specimen also could be adjusted by altering the diameter of the laser beam with the diaphragm. By irradiating the specimen and then evaluating the laser-induced wound with a through-focal series, we concluded that the plane of focus of the UV microbeam was essentially indistinguishable from the plane of focus of the 488-nm imaging laser used by the Bio-Rad, scanning confocal imaging system. We made no attempts to measure the laser power at the specimen, but found, based on the severity of wounds induced, that it was highly reproducible from one experiment to the next.

In response to the laser, the cells were ablated and the mechanical continuity of the tissue, epidermis, leading edge, or amnioserosa was destroyed. This result was likely due to a combination of specific effects of the 337.1-nm light and some local heating (Greulich and Leitz, 1994). At high doses of the laser, a local bubble in the tissue appeared, visible by differential interference microscopy and consistent with cavitation due to local heating. Such doses were not used in these experiments. Under the conditions used in these experiments, cells adjacent to the site of irradiation appeared unaffected by the laser for the following reasons. First, there was no indication that the GFP-moesin we used to image the cells was bleached adjacent to the site of irradiation. Second, some-to-nearly complete recovery was apparent in most of the embryos imaged after wounding. In a number of cases, dorsal closure was complete and hatching ensued.

Image Handling

Typically, high resolution electronic images were captured by the COMOS (Bio-Rad Laboratories) imaging software using a 1–3× zoom, Kalman averaging (4–6 frames), and contrast stretching. Images were stored on the hard disk of the DOS/Microsoft Windows driven personal computer as TIFF files, transferred to a Macintosh OS8-based platform, and opened in Adobe PhotoShop or NIH Image (version 1.6.1; available at http://rsb.info.nih.gov/nih-image/) for further manipulation. For multipanel figures and labeling, PhotoShop or NIH Image images were montaged in Canvas (Deneba Software) or PhotoShop. Hard copies were printed at 600 dpi on an Apple Laser printer for work prints or Epson Stylus 3000 printer (for glossy, publication quality prints). For QuickTime movies (Apple Computer, Inc.), individual frames or stacks of frames were manipulated in NIH Image, made into a stack, and saved as a QuickTime movie.

To increase the temporal resolution with which images could be saved, we recorded the 1-Hz video output of the Bio-Rad COMOS–controlled scanning laser imaging system directly onto superVHS videotape using a Sony tape deck at standard video rate (model Sony SVO-9500MD). By irradiating the specimen at a particular time in the image scan cycle (i.e., so that the specimen was irradiated just before the scan of the confocal, imaging laser reached the site of ablation), temporal resolution was increased substantially (with a maximum of 1 Hz/512 scan lines per image = 2 μs). A time stamp was added to each frame recorded with a Horita SCT-50 time/date generator.

To analyze cell shape changes and tissue movements, video frames were digitized on a Silicon Graphics O2 workstation using the program Isee (Inovision Corp.). To reduce noise in these unfiltered images, eight frames were averaged. Such digitally enhanced images were stored as TIFF files and manipulated as described below. NIH Image was also used to make various measurements on time-lapsed records of dorsal closure. COMOS software was used to collect Kalman-filtered, contrast-stretched images, typically once every 30–60 s. Time-lapsed files from Bio-Rad COMOS were opened as a stack in NIH Image (width 768, height 512, and header 76) and manipulated using NIH Image software. Measurements were downloaded into Microsoft Excel and data were graphed using Excel utilities.

Analysis of Tissue Movements after Ablation

The Isee software used a cross-correlation algorithm to track the position of individual, brightly fluorescent points on images of the embryos digitized from the tape as described above. Typically, cellular junctions were selected because they could be identified unambiguously from frame to frame. These trajectories were further analyzed with Microsoft Excel; images displaying the trajectories were obtained using Silicon Graphics utilities and Adobe PhotoShop.

We evaluated the intrinsic or resting tension present in various epithelia in a semi-quantitative fashion by mapping the trajectory of points adjacent to the site of laser ablation as follows. Cells organized into structures such as tissues or organs have an inherent or resting tension that is partially responsible for the organ's shape (Van Essen, 1997). This tension changes in response to external forces as well as in response to internal forces generated during morphogenesis. In our preparations of *Dro-*

sophila embryos, external, mechanical forces are maintained constant, so any observed tension is characteristic of forces produced by embryonic cells and their interactions. The relationship between the displacement of the points and tissue stiffness or tension is addressed in Results.

All of the results reported here are based on observations done on at least three and usually many more embryos.

Supplemental Materials

Supplemental Figure 1. The annotated sequence of the sGMCA transgene in its P element vector.

Time-lapsed videos are available to further depict many of the figures in this paper.

Video 1. Time-lapsed view of Fig. 1 and starts with germ band retraction (gbr) and continues through to completion of dorsal closure (dc).

Video 2. The embryo in Fig. 3, a dorsal view of dorsal closure is shown.

Video 3. This video corresponds to Fig. 5 and shows at a higher magnification the change in the cell shape at the leading edge from the end of gbr through dc.

Video 4, 5, and 6. These videos correspond to Fig. 7 and show video records of wound formation and muturation in the leading edge of the lateral epidermis in three embryos, one of which is depicted in Fig. 7.

Video 7. This video corresponds to Fig. 9 (a and b) and shows a wound to the amnioserosa.

Videos 8 and 9. These videos show the embryos in Fig. 9 (e and f, respectively). These are examples of wounds to the lateral flank of the embryo during dc.

Videos 10 and 11. Time-lapsed views of Fig. 10 (a–e and f–j, respectively) show two and four wounds to the le during dc.

All supplemental materials are available at http://www.jcb.org/cgi/content/full/149/2/471/DC1.

Results

Imaging Cell Movements during Dorsal Closure

General Approach. To examine the forces that contribute to dorsal closure, we developed methods to image dorsal closure in vivo using a strategy that targets GFP to actin and, therefore, the actin-rich cell cortex (Edwards et al., 1997 and supplemental videos at http://www.jcb.org/cgi/content/full/149/2/471/DC1). We used P-transposable element technology to generate lines of transgenic flies with a chimeric construct that fused the ubiquitously expressed promoter/enhancer from the *spaghetti squash* gene (that encodes the nonmuscle myosin regulatory light chain) to drive the GFP fused to the autonomously folding actin binding region of fly moesin (subsequently referred to as

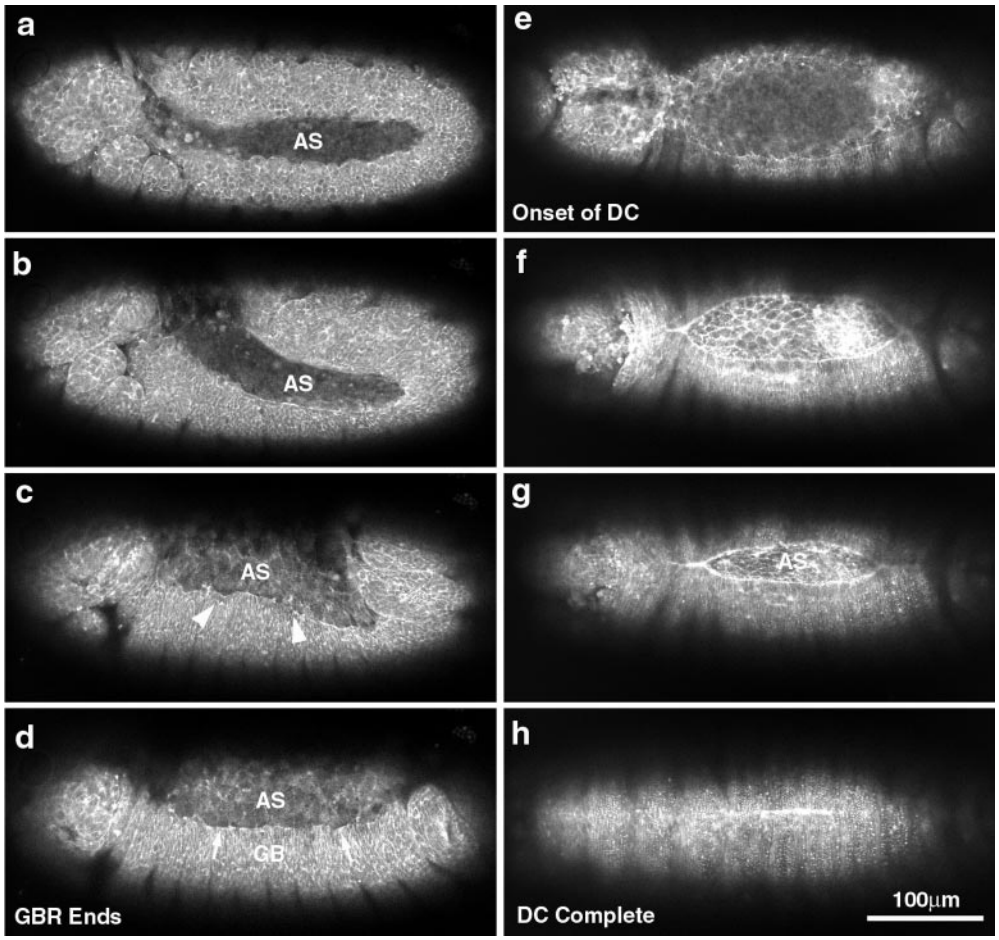

Figure 1. Low magnification micrographs of two embryos provide an overview of morphogenesis from extended germ band through dorsal closure. Two embryos with slightly different orientations give an overall view of the movements examined in this study (a–d, nearly sagittal view; and e–h, dorsal view). The posterior end of the germ band is indicated by arrows in a–c. (a) Germ band–extended embryo. (b) Germ band retraction has begun. The amnioserosa is indicated (AS; time, 54 min since a). (c) Germ band retraction, 80–90% complete (time, 1 h 21 min since a). The leading edge of the lateral epidermis has not yet accumulated much actin and is irregularly shaped (c, arrowheads). (d) Germ band retraction is essentially complete (time, 1 h 51 min since a). The leading edge of the lateral epidermis has begun to accumulate more actin in local regions (d, arrows). (e) End of germ band retraction, beginning of dorsal closure. The stage here is approximately the same as shown in d. (f) Dorsal closure is 50–75% complete. The leading edge of the lateral epidermis is resolved into a smoothly arcing front and appears as a bright line, indicating that it has begun to accumulate more actin (time, 2 h 33 min since e). (g) Dorsal closure 80–90% done. Even at low magnification, the change in cell shape from polygonal, at the end of germ band retraction, to elongate at this stage of dorsal closure is apparent. This is seen in the lateral epidermis (elongated perpendicular to the long axis of the embryo) and in the amnioserosa (elongated parallel to the long axis of the embryo; time, 3 h 9 min from e). (h) Dorsal closure complete. The bright bar indicates that the embryo just finished closing. In later panels (not shown), no scar is observed. Bright spots are denticles. A 25×, 0.8 NA lens was used to collect these images. Bar, 100 μm.

sGMCA). We mounted sGMCA embryos in gas-permeable observation chambers and observed their development with high numerical aperture objectives. The observation chambers allow high resolution time-lapsed imaging by scanning confocal microscopy with >95% of sGMCA embryos mounted before dorsal closure stages surviving through to hatching and beyond.

We focus on embryogenesis from the end of germ band shortening and the onset of dorsal closure to the completion of dorsal closure; we use this part of Results to detail the structure of the embryo during this time period. This phase of embryogenesis spans stage 13 to the end of stage 15 and at 25°C corresponds to ~9.3 h to ~13 h, respectively, after egg lay (note, however, that our experiments were performed at room temperature, ~20–23°C on embryos typically aged overnight at 18°C). The staging and morphology of the embryo are described in detail for both living specimens and fixed and sectioned material in Campos-Ortega and Hartenstein (1997; see pages 72–86), and has been studied by scanning electron microscopy (Turner and Mahowald, 1977, 1979) and is documented in this study by video time-lapsed analysis. (See also Flybase at http://flybase.bio.indiana.edu:82/images/lk/Animation/gastrulation-dorsal.mpg.)

Low Magnification Overview and Nomenclature. Fig. 1 presents a panel of images from time-lapsed sequences of sGMCA embryos that are otherwise wild-type. Corresponding time-lapsed sequences appear at http://www.jcb.org/cgi/content/full/149/2/471/DC1. Fig. 2 presents a schematic of the cross-section of the embryo during middorsal closure stages (late stage 14). The images demonstrate the overall changes in embryo shape from germ band retraction through dorsal closure (Fig. 1) and put the cell sheet morphogenesis that is the focus of this study in perspective (for review of overall changes in embryo structure see Wieschaus and Nusslein-Volhard, 1986 and Campos-Ortega and Hartenstein, 1985, 1997). The elongated, extended germ band shortens to 50–60% of its extended length (Fig. 1, a–d, arrows indicate posterior end of germ band). Initially, the amnioserosa is a bilaterally symmetric strip of tissue: on either flank its posterior-most end is cupped by the extended germ band. The amnioserosa extends anteriorwards to ~67–75% egg length, where it arcs dorsally to the embryonic midline (AS in Fig. 1, a and b). Once the germ band shortens to its full extent, the amnioserosa covers a large part of the dorsal surface of the embryo. The canoe-shaped cuboidal to columnar epithelium that constitutes the germ band occupies the ventral surface and arcs dorsally at either embryonic pole. The process of dorsal closure occurs when the lateral epidermis expands dorsally to envelop the amnioserosa (Fig. 1, e–h).

For clarity, we define several relevant structures or components of the embryo that are likely to contribute in distinct ways to the process of dorsal closure (Fig. 2 a). The leading edge of the lateral epidermis or leading edge is the dorsal-most part of the epidermis, and literally leads the lateral epidermis in its movement toward the dorsal midline. This leading edge of the lateral epidermis is a part of the leading edge cells or cells of the leading edge, which formally consist of the single, dorsal-most row of cells in the lateral epidermis. We use the more generic term lateral epidermis to refer to the epidermis and the cells more ventral to or behind the leading edge cells. We refer to the ventral-most part of the epithelium as ventral epidermis.

Structural Considerations. For a large part of the dorsal closure, the embryo remains structurally simple and amenable to approaches designed to evaluate the distribution of forces required for dorsal closure as follows. First, essentially all of the ectoderm that covers the entire surface is a simple (i.e., single cell layer thick) epithelium. The

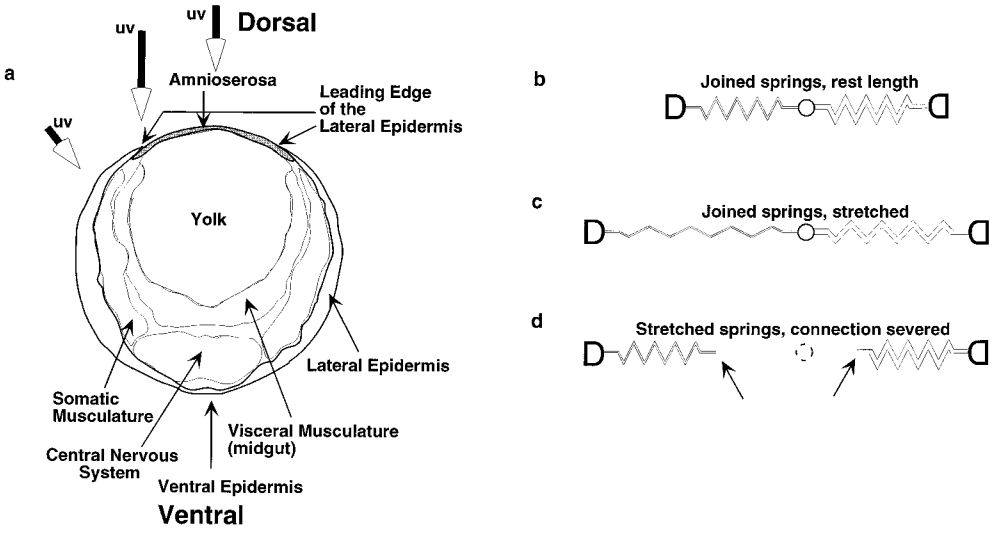

Figure 2. Schematic of tissue organization and simplified analysis of intrinsic tension/stiffness. (a) Schematic of embryo at early dorsal closure (traced from Campos-Ortega, 1985 Fig. 3.8A). Tissues and structures referred to in the text are appropriately labeled. Large arrows depict the beam of the irradiating laser for ablation of cells in the lateral epidermis, the leading edge of the lateral epidermis and the amnioserosa. Note that, at these early stages, the leading edge of the lateral epidermis and the amnioserosa overlie yolk (see text). (b–d) Schematic diagrams depict idealized, Hookean behavior (i.e., conforms to Hooke's Law) of a tissue. b shows an idealized tissue that varies in stiffness. Thus, the spring constant (or stiffness) of the spring to the left is half that of the one on the right. Shown are the springs at rest length, i.e., there is no intrinsic tension. c shows the ideal tissue with tension applied across it. Note that the stiffer tissue (spring) on the right extends half as much as the tissue (spring) on the left. This is because the tension across these two tissues in series is identical and, because $F = kx$ and $x = F/k$, the amount stretched (x) will be half for the stiffer spring. d shows what happens when the tissue is cut (here between the two springs) and the tissue on either side of the cut regains its equilibrium length. Note that the end of the spring on the left moves half as far as the one on the right (d, arrows, dotted circle indicates position of linkage before tissue cutting).

dorsal surface, except at the embryo ends, is covered by a simple squamous epithelium, the amnioserosa (Figs. 1 and 2; see Fig. 2.22 F, p.64; Fig. 2.30 B, p. 80; and Fig. 2.31, A–F, pp 81–83 in Campos-Ortega and Hartenstein, 1997). The remainder of the embryo is covered with a simple cuboidal to columnar epithelium. An exception to this simple epithelial structure occurs at the junction between the amnioserosa and the lateral epidermis where one or two cells of the lateral epidermis overlap one or two cells of the amnioserosa. The structure of this embryonic ectoderm and the two tissues of which it is comprised can be envisioned as a canoe or kayak with a canvas cover: the hull represents the lateral and ventral epidermis, and the canvas cover represents the amnioserosa. Indeed, a number of mutations in the dorsal closure have been named for the open boat phenotype that results when dorsal closure fails (e.g., *canoe*, *kayak*, *punt*; Jurgens et al., 1984). However, in contrast to a canvas cover, the amnioserosa tucks under, not over, the gunwales that define the canoe's cockpit. During dorsal closure, the lateral epidermis on each side spreads dorsally to meet at the dorsal midline (a dorsally closed canoe or kayak would never swamp, and with an appropriate ballast might function reasonably well as a submarine).

Second, the structure of the embryo suggests that the forces responsible for dorsal closure reside in the epithelia themselves and not in the tissues that underlie the epithelia. While multiple cell layers develop during gastrulation and neuroblast delamination, events that occurred earlier in embryogenesis, the endoderm and mesoderm are apposed to the ventral ectoderm except at the ends of the embryo (Fig. 2 a and figures from Campos-Ortega and Hartenstein, 1997 that were cited above). As a consequence, most if not all, of the amnioserosa overlies the yolk sack, a plasma membrane–bound bag that appears to have little if any mechanical integrity. An example of this lack of mechanical integrity occurs when an embryo is pierced with a micropipette; damage to the epithelium is local as would be expected for a puncture wound to a mechanically robust epithelium, but yolk flows freely out of the wound (data not shown). We conclude that the mechanical properties of the yolk sack do not contribute to dorsal closure. In concert with the dorsal closure of the epidermis proper, the midgut, formed initially of two parallel bands of cells that run along the flank of the embryo, closes around the yolk, both ventrally and dorsally. While in principle the mechanical integrity of the midgut is expected to be high, sectioned material and our own through-focal studies indicate that the midgut is 10–15 μm below the basal side of the lateral epidermis at the leading edge. As a consequence, it does not appear able to provide a substrate with which the cells of either the amnioserosa or the lateral epidermis can interact. Later, close contacts between the dorsal epithelium and underlying tissues may contribute to the mechanical stability of the epithelium (Rugendorff et al., 1994), but such contacts appear to form only at the end of dorsal closure.

Finally, the ectoderm has little if any mechanical connection to the vitelline envelope that surrounds the embryo as evidenced by the following. The vitelline envelope is the tough, proteinaceous and flexible egg shell in which the embryo lives until hatching, at which time the embryo rips its way through the anterior end. During stage 15 and later, body wall muscle contractility drives the movement of the embryo within the vitelline envelope. These movements appear to occur in a completely unconstrained fashion, and are uncoupled from any observable deformation of the envelope (data not shown). Moreover, at earlier stages, this envelope can be ripped or torn with a micropipette and the embryo slides freely out without apparent resistance. Together, these observations lead us to conclude that forces that contribute to the bulk of the movements during dorsal closure must reside in the embryonic ectoderm.

Introduction to High Resolution Studies. To investigate how individual cell shape changes and rearrangements might contribute to these movements we have imaged sGMCA embryos at high resolution. Time-lapsed images of the amnioserosa, the lateral epidermis and the ventral epidermis during dorsal closure stages (stages 12–15; ~9–15 h after egg laying) reveal changes in the structure of the cell sheet that were not apparent from fixed and stained specimens. First, we describe cell shape changes observed in wild-type, unperturbed embryos. Time-lapsed videos can also be viewed at http://www.jcb.org/cgi/content/full/149/2/471/DC1. Documentation of the dynamic changes in cell shape at these stages of *Drosophila* embryogenesis has not been possible using standard light microscope methods on living embryos. Our images of cellular dynamics during dorsal closure stages in living embryos suggest that interpretation of the sequence of events that occur based on fixed specimens are not entirely correct. For example, the hypothetical time-lapsed sequence compiled from scanning electron micrographs provides an excellent overview of the changes in the morphology of the surface of the embryo during development and is available on Flybase (http://flybase.bio.indiana.edu:82/images/lk/Animation/gastrulation-dorsal.mpg). Nevertheless, it suggests that a residual opening persists long after our data show that normal embryos have closed dorsally. Despite the obvious inability of the images of fixed embryos to provide an accurate temporal record of changes, individual fixed images are completely consistent with the changes observed by our time-lapsed studies.

Cell Shape Changes in the Amnioserosa

The squamous epithelium that covers the dorsal side of the embryo constitutes the amnioserosa. It is composed of cells that are dynamic and change dramatically through the course of dorsal closure. Through-focus analysis indicates that the amnioserosa extends under the edge of the lateral epidermis by approximately one row of cells. Shape changes include a reduction in the area of the amnioserosal cells in the plane of the epithelium, a loss of cells from the plane of the amnioserosal epithelium, and decreases in cell width measured perpendicular to the long axis of the embryo. These changes are as follows. Individual cells or small clusters of cells undergo changes in shape and area that parallel changes in the overall shape of the amnioserosa exposed to view (Figs. 3 and 4). Time-lapsed sequences of the changes in the amnioserosa show that the apical surface of individual amnioserosal cells change at a rate that is identical to changes in the rate at which the am-

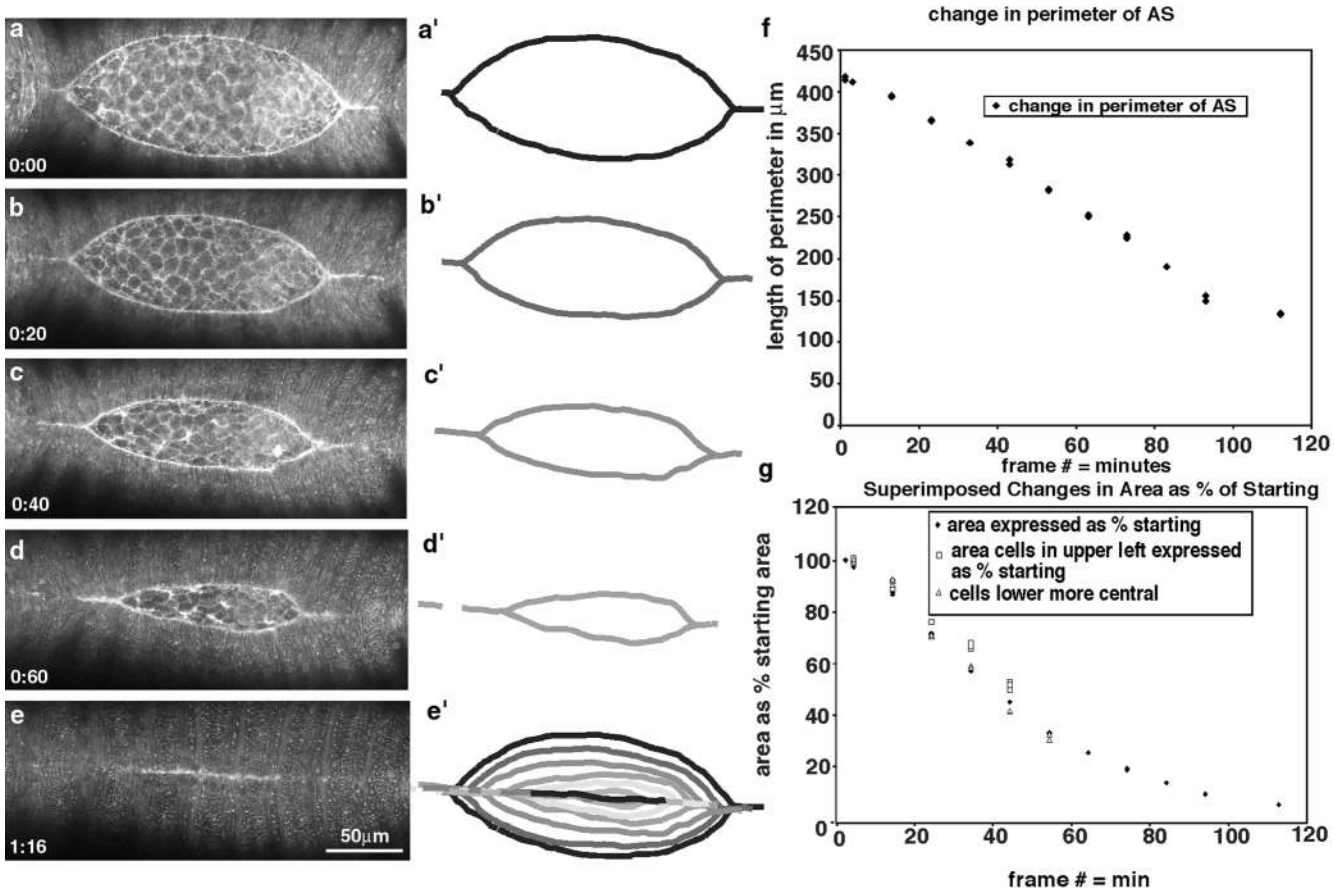

Figure 3. A dorsal view of cell shape change in dorsal closure. Overall changes in the shape of the leading edge of the lateral epidermis are shown in a–e and in schematic form in a′–e′. f plots the change in the length of the leading edge as it changes at time 0 (a) through to when it remains a bright bar of tightly apposed cells in e. Note that the length of the leading edge in e can also be interpreted as 0. The graph shows that a change in length is essentially linear with time. Analysis of the change in area (g) indicates that individual clusters of cells (open symbols) change area at the same rate as the amnioserosa disappears (solid triangles), implicating changes in the area of the amnioserosa with progress of the leading edge of the lateral epidermis (see text).

nioserosa, as a whole, changes shape (Fig. 3 g). In addition, individual cells of the amnioserosa drop out of the plane of the surface of the embryo and appear to pull adjoining cells over themselves as they do so (Fig. 4, arrows). This loss further contributes to a decrease in amnioserosal surface area. For example, in one case, during the course of dorsal closure 13 of the 110 cells in the amnioserosa drop out of the plane of the amnioserosa. Finally, in addition to the overall changes in the surface area of the apical ends of the amnioserosal cells, these cells change shape from being polygonal and essentially isomorphic to highly asymmetric. Initially, the average ratio of their length (measured perpendicular to the long axis of the embryo) to their width, measured parallel to the long axis of the embryo, is >2. By the end of dorsal closure, the ratio has decreased to 0.5 or less (Fig. 3).

These dynamic changes in the structure of the amnioserosa are inconsistent with our original model (and other models that were based on fixed specimens, e.g., Campos-Ortega and Hartenstein, 1985) in which it was hypothesized that the lateral epidermis passed over a passive and unchanging amnioserosa. In contrast, our observations agree with more recent observations from fixed and sectioned material (Rugendorff et al., 1994; Rickoll, W.L., and D.P. Kiehart, unpublished observations). Moreover, they are consistent with cell autonomous shape changes driven by contractility in the amnioserosa itself. We test this hypothesis more directly below.

Cell Shape Changes in the Lateral Epidermis and in the Leading Edge of the Lateral Epidermis

At the start of dorsal closure, cells throughout the lateral epidermis are polygonal in shape (Fig. 5 and supplemental video at http://www.jcb.org/cgi/content/full/149/2/471/DC1). At the leading edge, they are slightly elongated perpendicular to the long axis of the embryo. Early in dorsal closure, the interface between the leading edge and the amnioserosa is scalloped (Fig. 5 a). Moreover, time-lapsed analyses demonstrate that the exact position of the cells of the leading edge, their shape, and the position and shape of the cells of the amnioserosa all appear to fluctuate. Thus, local regions of the scalloped, leading edge advance and retreat (see supplemental video at http://www.jcb.org/cgi/content/full/149/2/471/DC1). Initially, the concentration of actin at the leading edge appears comparable to

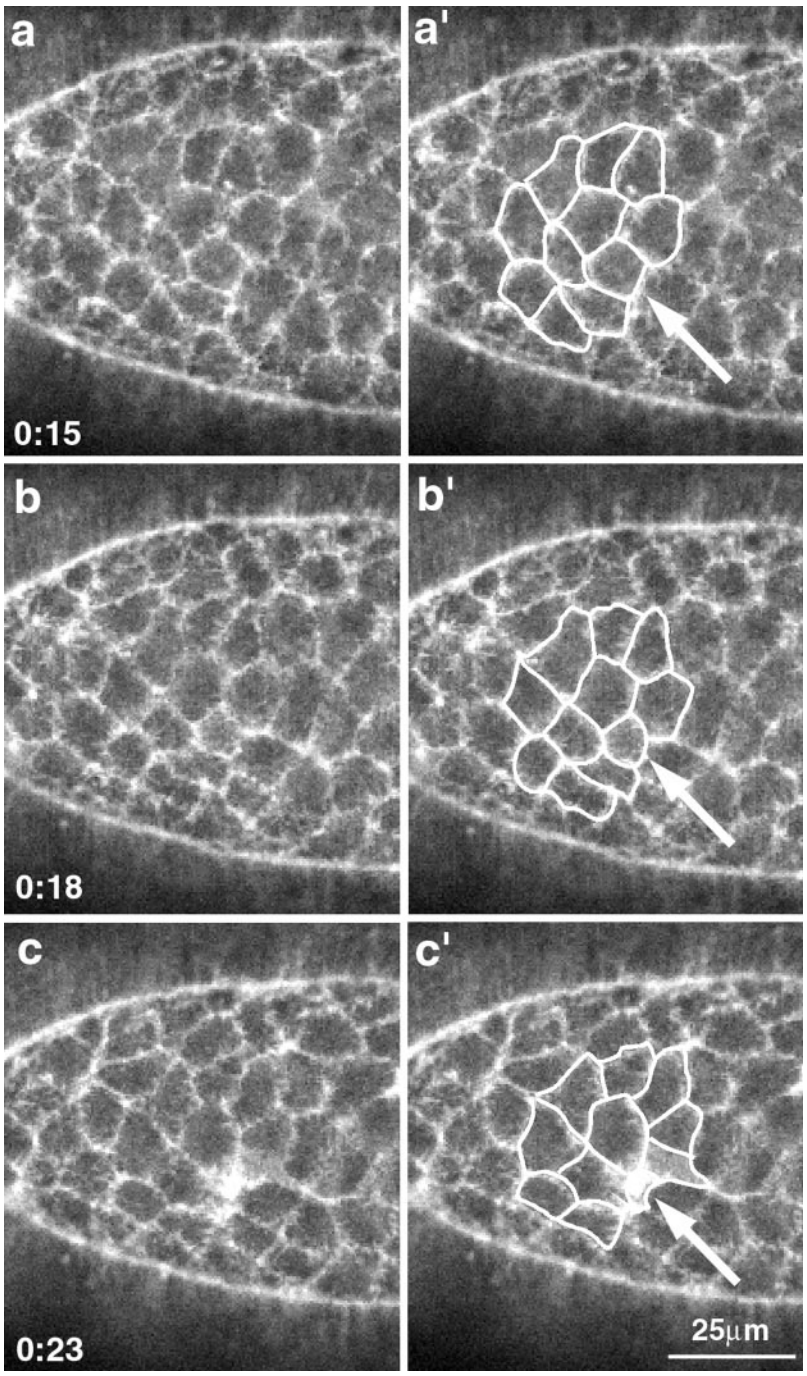

Figure 4. The amnioserosa loses cells during dorsal closure. A high magnification view of the amnioserosa shows a cell that accumulates actin at its apical end and drops out of the plane of the tissue (arrow). Time in minutes (from the start of the time-lapsed sequence) is shown in the lower left. a′–c′ are identical to a–c, but have a set of cells outlined in white to show the overall change in shape.

that at other cell margins. With time, scalloping at the leading edge smooths out, the leading edge resolves into a gently arcing, continuous band, and the fluorescence due to sGMCA at the leading edge increases, indicating that actin accumulates there. As dorsal closure proceeds, the cells of the lateral epidermis elongate in the direction of spreading to accommodate the increased surface area required to cover the amnioserosa (Fig. 5).

Dorsal closure proceeds as the leading edge of the lateral epidermis advances toward the dorsal midline (Figs. 1, 3, and 5). Cells toward the polar ends of the lateral epidermis reach the dorsal midline first and form a continuous epithelium. Thus, from the dorsal side, the free leading edge of the lateral epidermis (i.e., that not apposed to leading edge from the opposite flank of the embryo) is essentially lens shaped. During the course of dorsal closure, the perimeter of the lens (i.e., the total length of the visible interface between the lateral epidermis and the amnioserosa) decreases as the result of two distinct processes (Figs. 1, 3, and 5). The leading edge of individual cells shortens (presumably by active contraction, see below) and, as cells reach the dorsal midline, they become juxtaposed to the leading edge cells from the opposite flank and no longer visibly interface with amnioserosa. In the example shown in Fig. 3, the free leading edge changes in length from 420 to 0 μm in under 2 h. During a comparable inter-

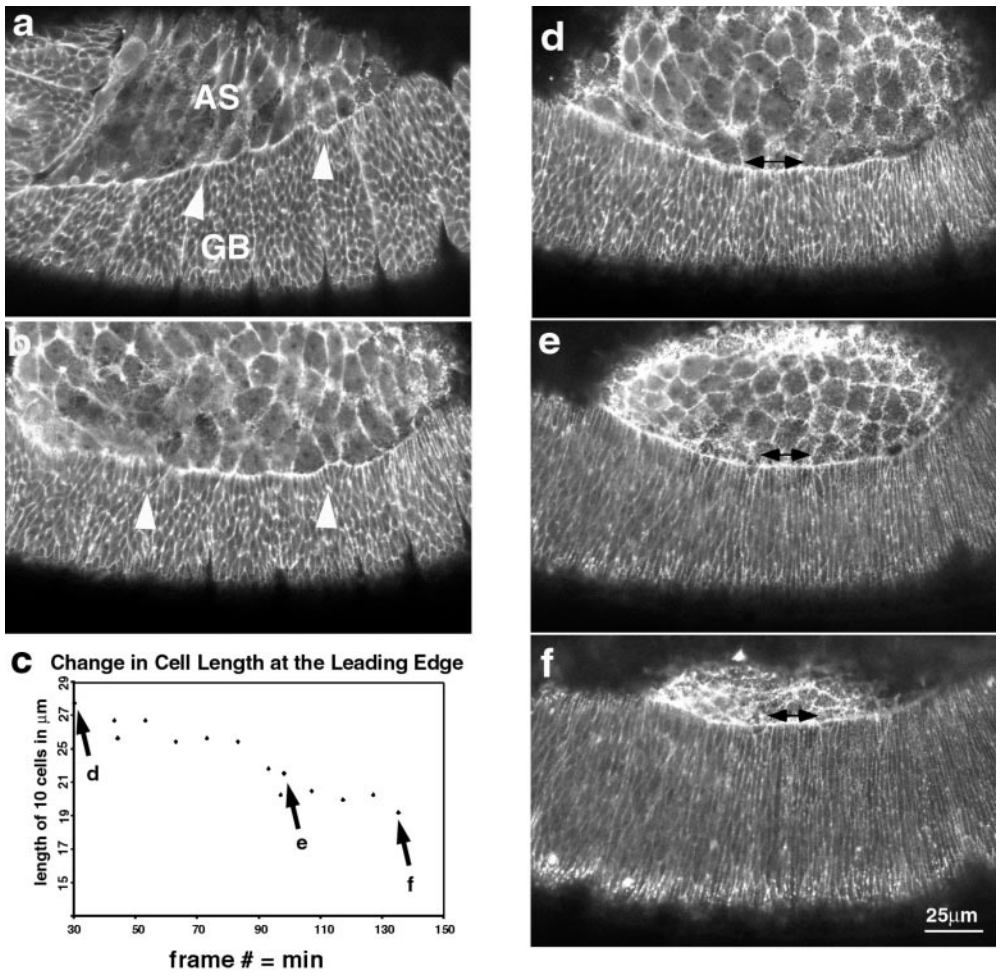

Figure 5. Changes in the lateral epidermal cell shape during dorsal closure stages show that the cells start off polygonal and become elongate. (a) Germ band (GB) retraction in progress (time is 5 min after the start of the time-lapsed sequence). Cells of the lateral epidermis (labeled GB) are polygonal in shape and the interface between the amnioserosa (AS) is scalloped (arrowhead). (b) Germ band retraction is complete. Arrowheads again depict scalloped edge (time is 61 min after the start of the time-lapsed sequence). (b) Graph of the length of the leading edge of the lateral epidermis marked by double-headed arrows in d–f. The abscissa of c represents the time for d minus 70 min. d–f are micrographs showing the elongation of the cells of the lateral epidermis (times are 104, 164, and 202 min after the start of the time-lapsed sequence). Double-headed arrows show the set of 10 cells whose overall length was reduced to ~68% of their original length during the course of the time-lapsed sequence shown. Points for each panel are labeled in c.

val, the average width of the leading edge of 10 cells changes from 28 to 21 μm (measured in another embryo at the posterior, middle, or anterior end of the dorsal opening; Fig. 5 e). The change in length is complex, with some clusters of cells shortening and others remaining longer at their leading edge (Fig. 5).

Analysis of the time-lapsed sequences indicates that the leading edge consists of a stable population of cells. We have not observed that cells drop out of the epithelium or migrate in the plane of the epithelium away from their position at the leading edge. Thus, cell rearrangements cannot explain the shortening of the leading edge during the dorsal closure process, and changes in cell shape must be responsible. Moreover, inspection of the time-lapsed video sequences reveals no indication of a flow of epithelial cells toward the poles, or any indication of forces that stretch the dorsal midline due to forces exerted at the poles.

What Kinds of Forces Contribute to Dorsal Closure?

Next, we used a biomechanical approach to investigate the forces that contribute to morphogenesis during dorsal closure. When cells grow and change their morphology, they cause an intrinsic or resting tension to develop within tissues and organs (see references in Discussion). At any given instant or when viewed over a sufficiently brief time interval, such forces or tensions are at apparent equilibrium (i.e., no movement is apparent). To investigate such tensions, we can perturb the equilibrium simply by cutting the tissue. This severing releases the intrinsic tension and the tissue springs open. To a first approximation, the behavior of the cut tissue can be modeled according to Hooke's law ($F = kx$, where F is the tension, k is the spring constant, and x is the displacement from the unloaded case; see Fig. 2, b–d). Consider two springs fastened at their ends and stretched. If the mechanical linkage between the springs is suddenly disrupted, the springs will shorten and assume a new, unloaded rest length. The net distance traveled by each new, free end will be proportional to how stretched the springs were (the tension, F) and the intrinsic stiffness of the springs (the spring constant, k). Real epithelia are not expected to behave in an ideal fashion because both the stiffness and the tension are likely to vary from point to point and over time. Nevertheless, it is reasonable to expect that both tension and stiffness are fairly constant in local regions of a homogeneous tissue like an epithelium and that displacement of wound edges directly after tissue ablation is a good measure of the mechanical properties of the tissue. Below, we refer to

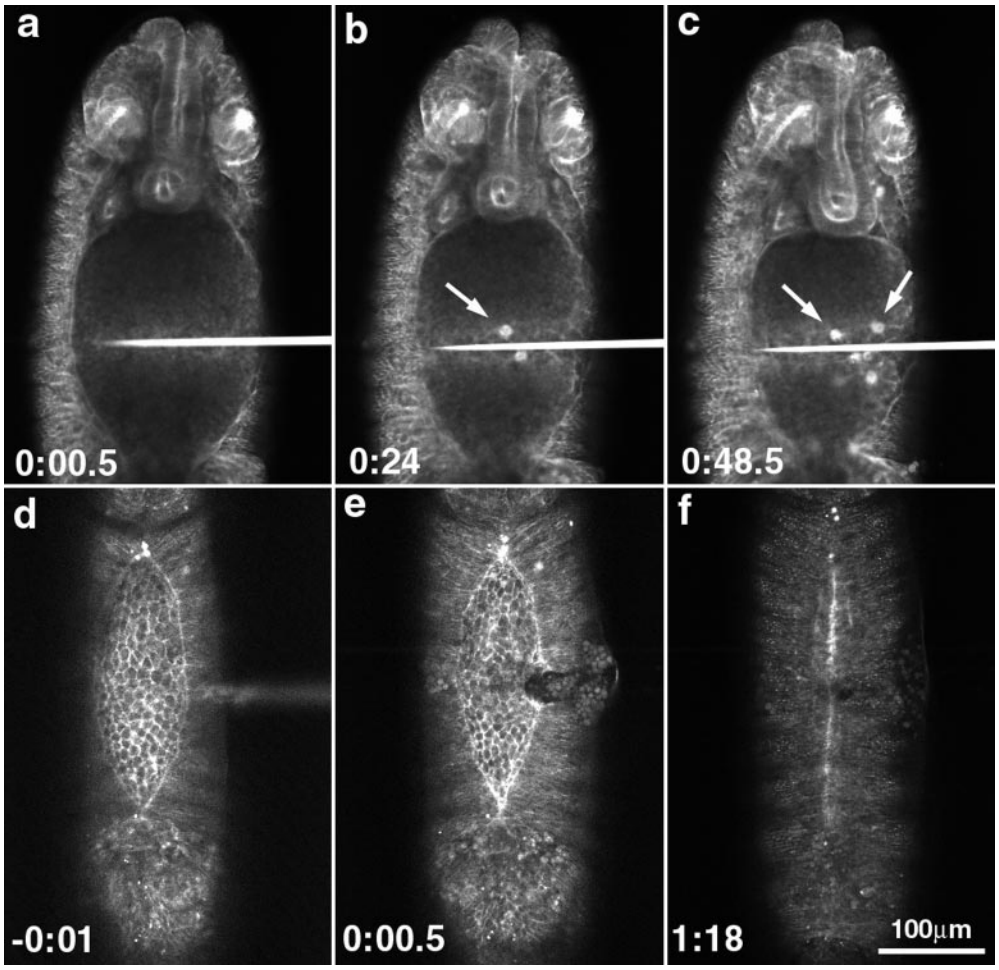

Figure 6. Mechanical wounds to the leading edge of the lateral epidermis cause hemocytes to accumulate and can disrupt the actin-rich supracellular purse-string. (a–c) Early dorsal closure–staged embryo with a micropipette inserted into its flank. Time is shown in minutes after insertion of the micropipette. With time, hemocytes begin to accumulate (b and c, arrowheads) as a response to wounding. (d–f) Before, right after, and after healing of a mechanically induced lesion in the leading edge of the lateral epidermis. Time is shown in minutes with respect to insertion of the micropipette. In d, the intact leading edge is shown, with the fluorescently filled micropipette out of focus and coming in horizontally from the right, just above the center of the panel. (e) After wounding, the leading edge is disrupted. (f) With time, the wound heals and dorsal closure is completed.

the stiffness/tension of the tissue because of the manner in which these two parameters are so closely linked.

Recall that we hypothesized that a supracellular, contractile actomyosin purse-string was responsible for the movements of the lateral epidermis during dorsal closure. A prediction of this model is that the leading edge is under tension and should behave like the connected springs described above and in Fig. 2, b–d. To investigate the contractile nature of the leading edge and other parts of the embryo, we devised methods to cut the tissues, observe, and record rapid changes in cell shape and position in the tissue adjacent to the cut.

Mechanical Wounding

To examine the mechanical properties of the leading edge, we first attempted to cut the lateral epidermis with a fine micropipette (Fig. 6). We subsequently abandoned this strategy because the lesions we produced were not sufficiently reproducible. Nevertheless, we show images of the mechanical wound to establish that the laser wounds we induce (see below) closely mimic mechanical lesions. Frequently, mechanical damage to the leading edge (and presumably to surrounding tissue) came only after the pipette was repeatedly removed and inserted in a saw-like fashion. A number of embryos went on to repair the wounds in the leading edge of the lateral epidermis, and then continued through dorsal closure and hatched. An interesting feature of the mechanical wound that accompanies insertion of the micropipette into the tissue is that hemocytes begin to accumulate around the site of the wound (Fig. 6, b and c, arrows). Because we could not cut the leading edge reproducibly with this method, we sought an alternative approach to cutting the tissue.

Laser Ablation

Laser ablation reproducibly cuts the epidermis. Like the mechanical wounds described above, these laser wounds heal and embryogenesis proceeds to hatching and beyond (see below). A short pulse of ultraviolet UV light induces a relatively circular lesion in uniform epidermal tissue within 10 μs (Fig. 7; see Materials and Methods). The nature of the laser-induced wounds depends on a number of factors including the intensity of the light and the number of pulses delivered. We can reproducibly ablate a small number of cells in a precisely targeted region of the embryo (e.g., see the laser induced lesions in the four different embryos targeted at the leading edge of the lateral epidermis shown in Figs. 7 and 8).

Upon irradiation of the leading edge of the lateral epidermis (Fig. 7 a, arrowheads), the tissue immediately be-

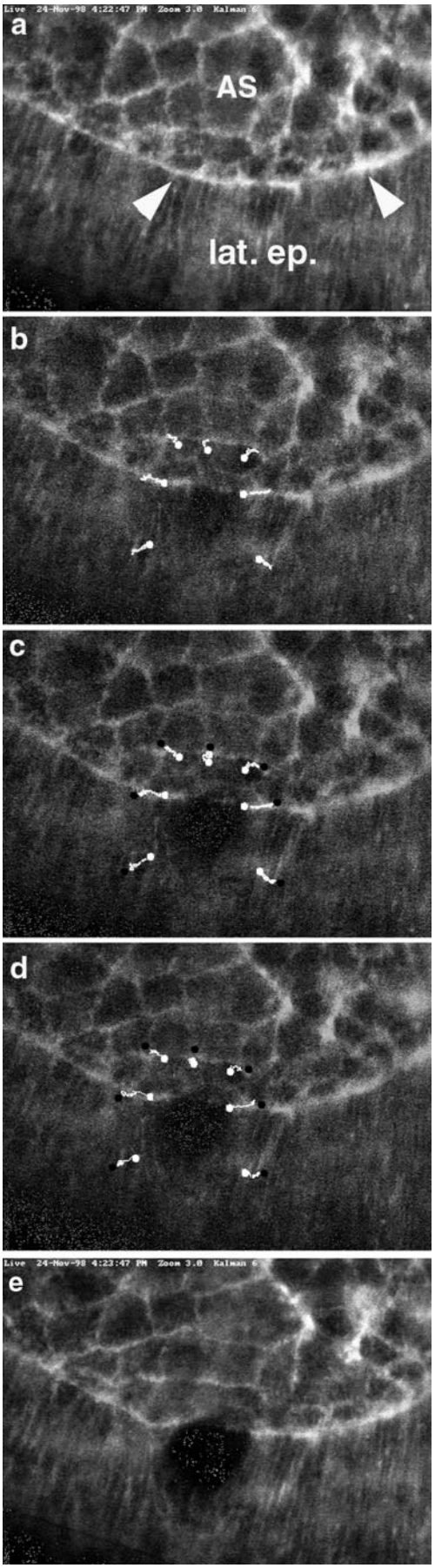

gins to spread (Fig. 7, b–d). Frame-by-frame analysis of the cells at the leading edge after laser irradiation shows that as few as two to three cells disappear or are ablated essentially instantaneously (within the time required by the imaging device to refresh the screen). In Fig. 7, approximately six cells were ablated (compare a and b). The confocal laser scanning system refreshes the image at ~1 Hz, so the first image after ablation appears after the 3-ns pulse at some variable time that is <1 s. Subsequent frames show that one or two additional cells adjacent to the wound fail with times that range from seconds to tens of seconds. Our interpretation is that they are either ripped apart by mechanical or thermal forces, experience lower levels of UV light, and are ablated more slowly, or a combination of all of these factors. We find that the diameter of the ablating spot is in excellent agreement with the size of bleached GFP fluorescence and/or wounds generated in stable tissue that is not actively rearranging and does not move after irradiation (data not shown). As described below, the wound continues to change shape for 30–75 s without further loss of cells. This spreading is presumably due to tension in the cell sheets (Figs. 2 and 7; see also supplemental videos at http://www.jcb.org/cgi/content/full/149/2/471/DC1).

Additional experiments showed that the extent of wounding was dependent on the dose of laser light delivered, and that tissues positioned 15 μm below the focus of the ablating beam were unaffected by the irradiation (data not shown). Because of the overall structure of the embryo, our interpretation is that the laser affects the surface epithelium, the underlying yolk, and little else (Fig. 2; see also description of embryo structure above). We also found that the extent of the wound for a given laser dose varied as a function of developmental time during dorsal closure. Very early in dorsal closure, wounding required low doses of UV light. By late in dorsal closure, the tissue stabilized and was resistant to laser ablation. During the middle of the dorsal closure stages, the effects of a given laser dose were reproducible (compare the irradiated embryos shown in Figs. 7 and 8), and a single pulse of laser light was typically used to cause the wounds.

The Leading Edge Is under Tension

Ablation of the actin-rich, purse-string–like band at the leading edge of the lateral epidermis demonstrates that the leading edge is under tension. It behaves precisely as predicted by our model for a contractile, supracellular purse-string (Figs. 7 and 8). Recall that our model was

Figure 7. Rapid changes in the leading edge after laser ablation demonstrate that actin and myosin at the leading edge of the lateral epidermis form a contractile purse-string that is under tension. (a) Kalman-filtered image of the embryo just before laser ablation. (b–d) Frames from videotape of the ablation taken 10, 20, and 40 s after a single 3-ns pulse of UV irradiation. White lines show the position of landmark points in the image as the tissue spreads in response to the wound. Note that the longest traces are those that track the position of points in the leading edge. There is minimal change in the architecture of the amnioserosa. The lateral epidermis moves an intermediate amount. e is a Kalman-filtered image taken after the wound stabilized.

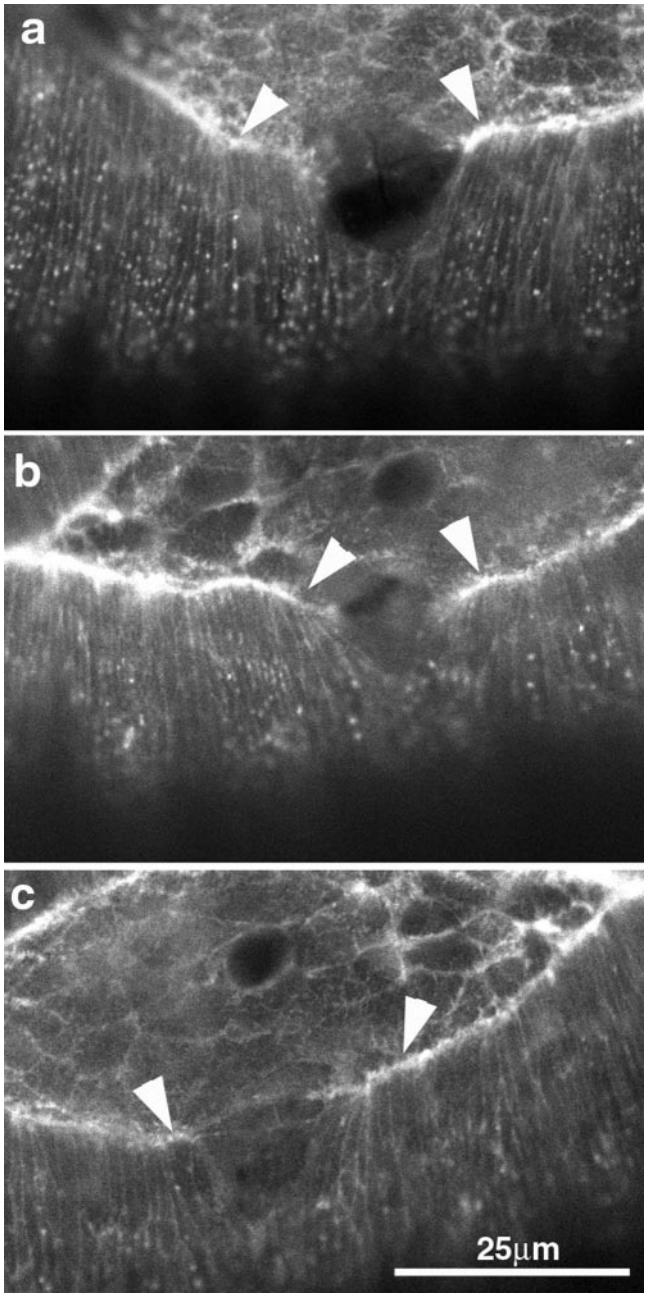

Figure 8. Reproducibility of the wounding process is demonstrated by this panel of three different embryos wounded at the leading edge of the lateral epidermis. Arrowheads indicate part of the leading edge that recoiled away from the site of laser irradiation.

based on our observation that embryos depleted of the myosin II heavy chain encoded by the *zipper* gene fail to properly execute dorsal closure (Young et al., 1993). Because of the distribution of myosin and actin in a supracellular purse-string–like band at the very leading edge, we proposed that dorsal closure could be explained through contraction of the band. Our model suggested that contractility at the leading edge would physically drag the lateral epidermis up and over the amnioserosa.

Rapid changes in tissue architecture after UV irradiation suggest that the leading edge is especially contractile. Irradiations targeted such that they cut or ablate the fluorescent contractile band at the very leading edge cause regions of the band adjacent to the cut to recoil or spring away from the site of irradiation. Before irradiation, the lateral margins of the leading edge cells are seen to be parallel to one another and perpendicular to the leading edge of the lateral epidermis all along its interface with the amnioserosa. After irradiation, cells spring apart, leaving the lateral margins of the cells adjacent to the wound slanted toward the embryo poles (Fig. 8, arrowheads). Moreover, the leading edge adjacent to the wound contracts and tends to move ventrally, away from the dorsal midline (Fig. 8 b). Contraction can be clearly observed in Figs. 7 and 8 (arrowheads indicate contracted cells). Real-time videotapes of the wounds indicate that the wound stabilizes (i.e., undergoes no further movements) in ~30–75 s (see supplemental video at http://www.jcb.org/cgi/content/full/149/2/471/DC1). Typically, we record a high resolution, averaged image once the cells stabilize and begin time-lapsed analysis of the wound healing process (Fig. 7 e, see below).

The exceptional contractile nature of the supracellular purse-string is also seen when both the leading edge and adjacent cells in the amnioserosa are targeted. We analyzed these movements in a semi-quantitative fashion by tracking the position of points adjacent to the site of irradiation after laser ablation (see Materials and Methods). The trajectory of points that describes recoil of the leading edge is typically longer than the trajectories describing recoil of the adjacent amnioserosa or lateral epidermis (Fig. 7, b–d). The special mechanical role of the purse-string in the leading edge is further supported by the observation that ablation of the leading edge cells, (but not the leading edge purse-string per se) frequently killed the cells but left the purse-string intact, at least transiently (data not shown).

Other Embryonic Tissues Are also under Tension

After laser ablation of the leading edge, analysis of the trajectory of points in both the amnioserosa and the lateral epidermis suggest that both tissues are also under tension, albeit less than that of the leading edge. There are a few exceptions in which one, or a small subset of points in the amnioserosa of a given embryo, recoils more than some of the points in the lateral epidermis (data not shown). Coupled with our observation that cell shape changes in the amnioserosa appeared to be cell autonomous, the stiffness/tension we observe suggests alternative and testable mechanisms for force generation during dorsal closure.

To investigate how tension in other regions of the embryo might contribute to dorsal closure and to provide a control for irradiations of the leading edge, we used the UV laser to ablate cells in other parts of the embryo. As described below, we found that, during dorsal closure stages, all lateral and dorsal aspects of the surface of the embryo were under tension.

Amnioserosa

Direct irradiation of the amnioserosa demonstrates that this tissue is also under tension. When the amnioserosa is

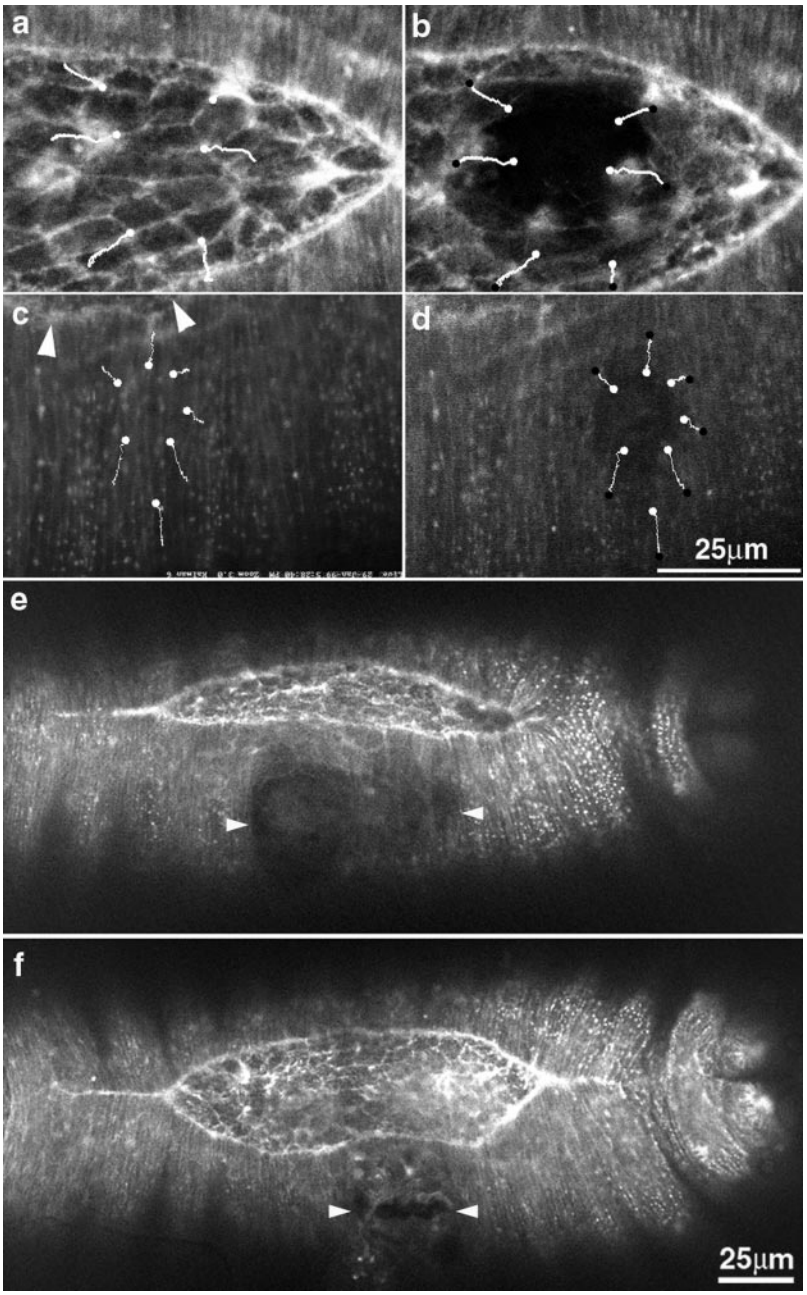

Figure 9. Wounding the amnioserosa and the lateral epidermis. (a and b) The amnioserosa shown before (a) and after (b) laser wounding. Note that the tissues surrounding the wound site spread outward, away from the wound, indicating that the tissue is under isotropic tension. (c and d) The lateral epidermis before (c) and after (d) wounding. Here, the spread of the tissue is anisotropic. In each case, white lines indicate the trajectory of points in the tissue after the irradiation. White dots mark the starting point and black dots mark the end point of the formation of a mature wound before the initiation of healing. Arrowheads indicate the location of part of the leading edge. (e and f) Multiple wounds to the flank of the lateral epidermis cause the leading edge to advance toward the dorsal midline. Arrowheads mark the lateral extent of the wounds, and are positioned to indicate the middle of the wound measured along the dorsal-ventral axis. As a consequence of the ablations, the leading edge of the lateral epidermis has prematurely advanced toward the dorsal midline. Bar for a–d is shown in d; bar for e and f is shown in f.

irradiated, individual cells or clusters of cells are ablated, and the tissue spreads (or opens) isotropically away from the site of the irradiation and the ablated and damaged cells (Fig. 9, a and b). The lateral epidermis appears firmly attached to the amnioserosa and spreads with it. These data are consistent with structural studies of fixed and sectioned material that indicate the amnioserosa cells change shape during dorsal closure and closely contact the lateral epidermis (Rugendorff et al., 1994, and Rickoll, W.L., and D.P. Kiehart, unpublished observations).

Lateral Epidermis

The lateral epidermis is also under tension (Fig. 9, c and d, arrowheads depict the position of the leading edge, part of which is just in view). When cells two or three rows ventral to the leading edge cells are irradiated with the UV laser, the cell sheet again spreads or relaxes away from the ablated or damaged cells. In contrast to the amnioserosa, spreading is anisotropic, suggesting that tension within the lateral epidermis is not uniform. Thus, movement of points ventral to the site of ablation is more extensive than movement both anterior or posterior to the site of ablation. Movements dorsal to the wound appear to be intermediate in magnitude. Interestingly, the lateral epidermis can bulge towards the dorsal midline and push into the amnioserosa. Thus, tension in the lateral epidermis apparently retards the forward progress of the leading edge. This condition is confirmed by the observation that the leading edge can be accelerated toward the dorsal midline by using successive laser ablations to wound a slit in the lateral epidermis (Fig. 9, e and f). Under these conditions,

the lateral epidermis arrives at the dorsal midline minutes after ablation, and remains there as the opposite flank of the embryo continues to close (Fig. 9, e and f; see also supplemental videos at http://www.jcb.org/cgi/content/full/149/2/471/DC1).

When the ventral epidermis is wounded during dorsal closure stages, it remains essentially inert (data not shown). This result contrasts our observations on the lateral epidermis, the leading edge cells, and the amnioserosa. Even when high doses of laser light are used to ablate ventral epidermis, the tissue does not spread. One possibility is that this point of zero tension is a consequence of the symmetry of the embryo and a balance of the ventrally directed forces that pull on either flank of the lateral epidermis (and retard its progress toward the dorsal midline, see above). Alternatively, the ventral epidermis may not be under tension because it is stabilized by interactions with the ventral nerve cord or with the extracellular matrix (precursors of the cuticle).

Embryonic Tissues Heal Rapidly after Laser-induced Wounding

Time-lapsed imaging reveals that laser-wounded tissues heal rapidly (over the course of minutes or tens of minutes; Fig. 10). After the initial development of a mature wound (30–75 s), the wound stops opening, appears to stabilize, and immediately begins to heal. Initially, there is lit-

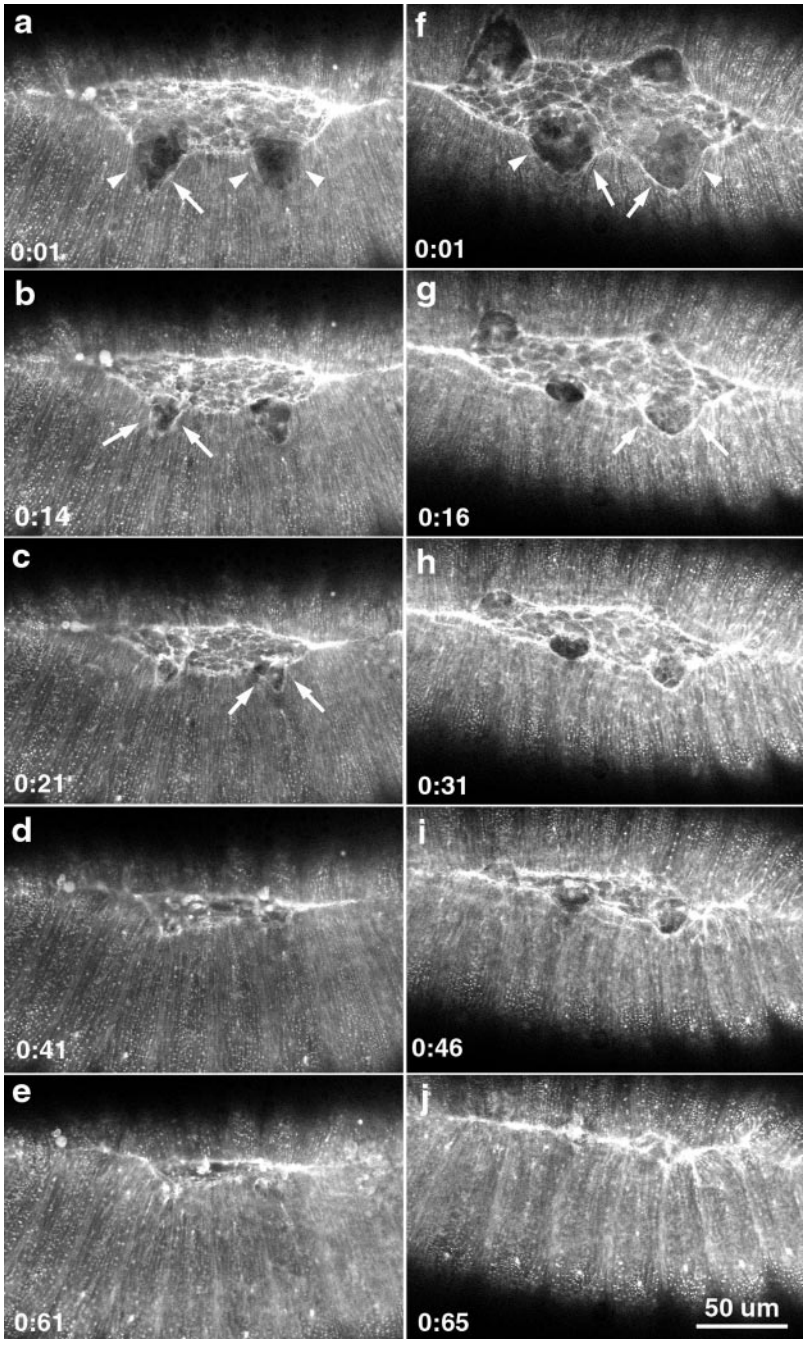

Figure 10. Recovery of the embryo after two and four wounds to the leading edge. a–e show a time-lapsed sequence of healing following two wounds to the leading edge. f–j show a similar sequence following 4 wounds to the leading edge. Arrowheads in a and f indicate the edges of the wounded lateral epidermis. Arrows in a–c, f, and g point to the accumulated actin at the site of the wound, indicating the formation of a purse-string response to wounding.

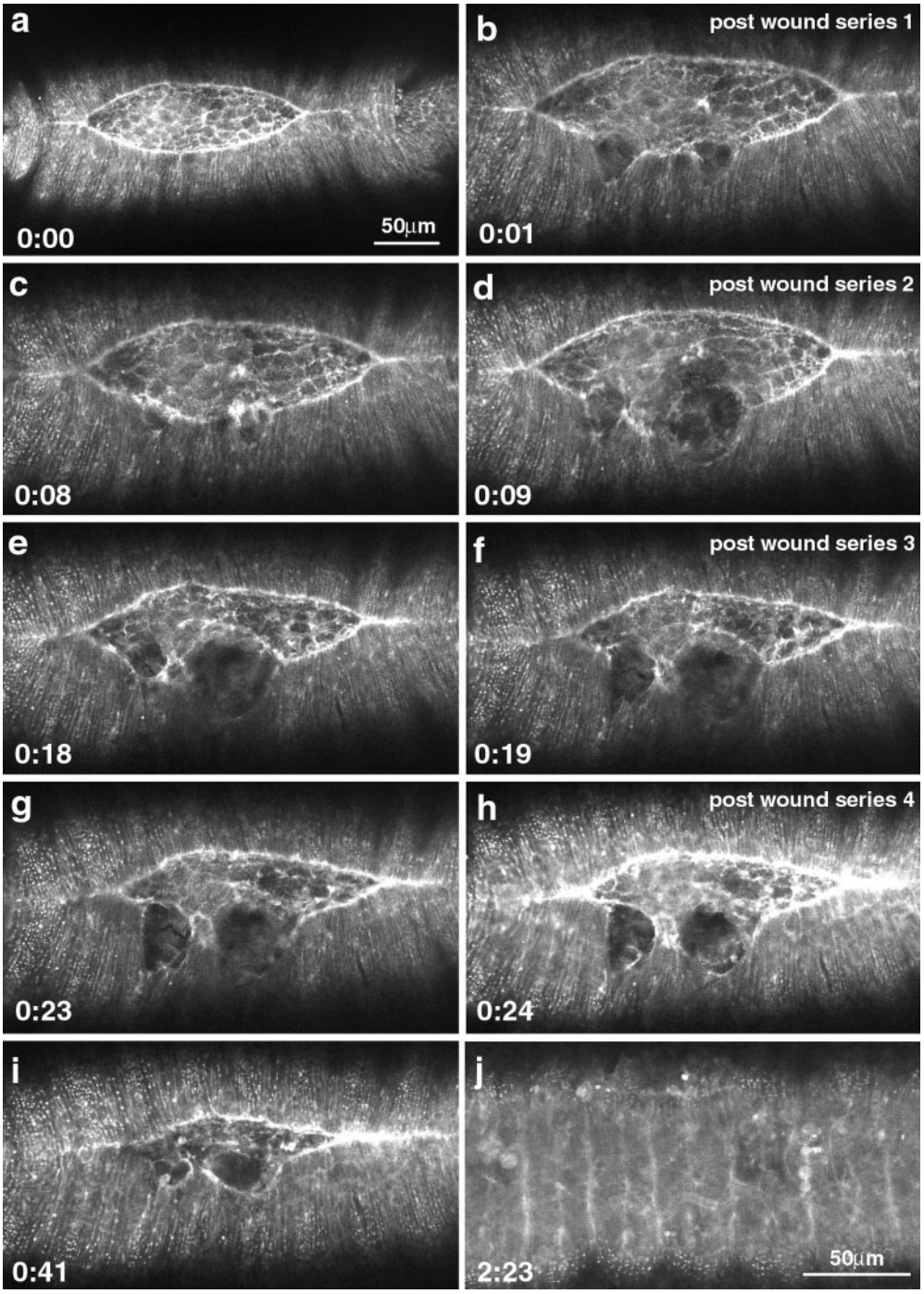

Figure 11. Repeated wounding of the leading edge does not stop dorsal closure. The leading edge was wounded as soon as healing was apparent (as observed by a through-focus analysis). Time is shown from the first panel in hours/minutes. The left column of panels shows the embryo just before wounding. The right panel shows the embryo after the first wound (b) and after subsequent wounds designed to disrupt the mechanical integrity of the leading edge.

tle actin at the newly formed wound margin (Fig. 10, a, b, f, and g, arrowheads), but within minutes actin is recruited to the wound margins (Fig. 10, a and f, arrows). Note, actin has already begun to accumulate at some wound margins (Fig. 10, a and f). Finally, through-focal series demonstrate that a new, actin-rich, wound purse-string extends completely around the wound, crossing the boundary between lateral epidermis and amnioserosa (b, arrows, and data not shown). This purse-string appears contractile because its circumference is rapidly reduced as the lesion in the epidermis closes and thereby heals (compare a and b to g and h; also see supplemental videos at http://www.jcb.org/cgi/content/full/149/2/471/DC1). This purse-string is reminiscent both of the supracellular purse-string that we described for dorsal closure (Young et al., 1993; and this work) and the purse-strings described for wounds in other systems (Martin and Lewis, 1992; Bement et al., 1993, 1999; Brock et al., 1996; Martin, 1997; for review of purse-strings see Kiehart, 1999).

Multiple Wounds Compromise the Mechanical Integrity of the Leading Edge and the Amnioserosa but Fail to Block Dorsal Closure

The spreading of the leading edge of the lateral epidermis away from sites of ablation, when either the leading edge

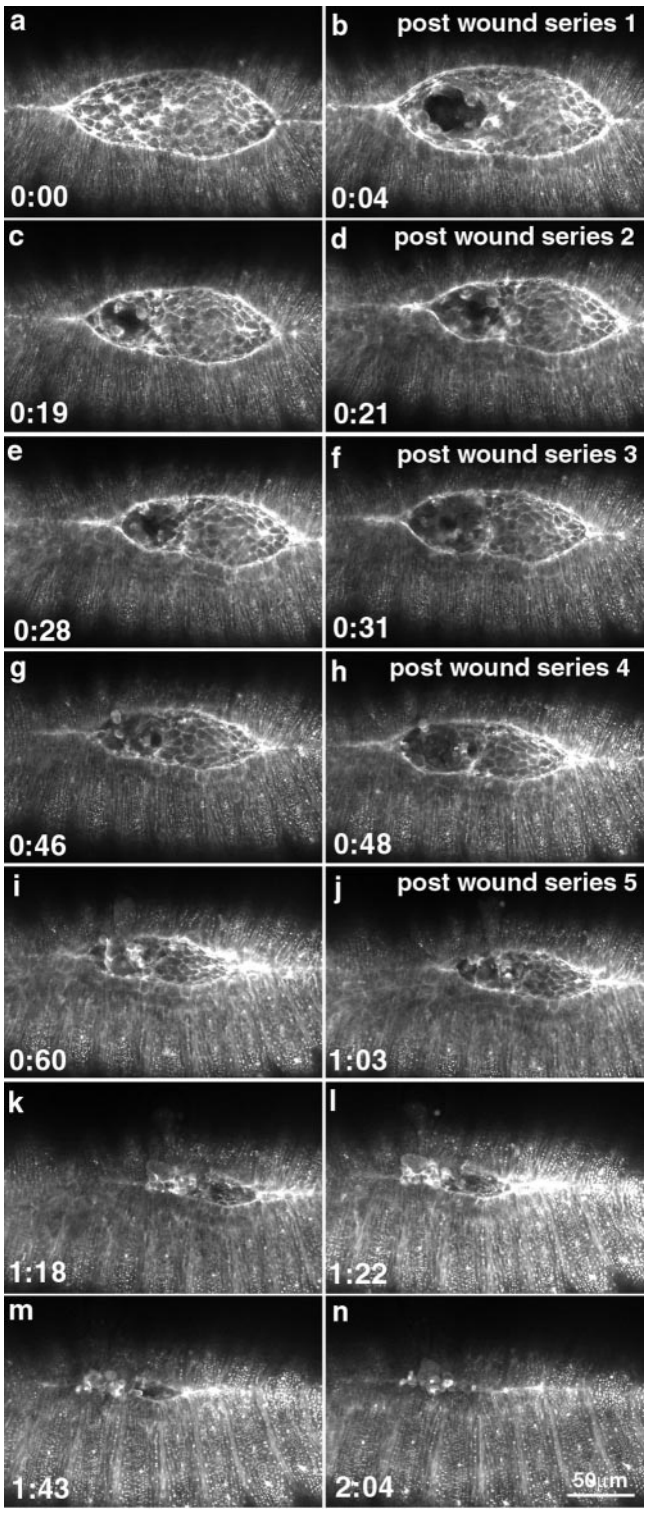

Figure 12. Repeated wounding of the amnioserosa does not stop dorsal closure. The amnioserosa was wounded as soon as healing was apparent (as observed by a through-focus analysis). The time is shown from the first panel in hours/minutes. The left column shows the embryo just before wounding. The right column shows the embryo after the first wound (b) and after subsequent wounds designed to disrupt the mechanical integrity of the leading edge.

(Figs. 7 and 8) or the amnioserosa (Fig. 9) are targeted by laser ablation, suggested that contractility of both tissues may contribute to cell sheet morphogenesis in dorsal closure. Certainly, the retreat of the leading edge away from the dorsal midline, as a consequence of ablation of either tissue, was consistent with this notion. In addition, the ability of the embryonic epidermis to heal itself was remarkable (see above) and, as a consequence, we could not rule out the possibility that after a single wound, the leading edge of the lateral epidermis or the amnioserosa healed and proceeded to drive dorsal closure. To test this hypothesis, we repeatedly irradiated the leading edge or the amnioserosa, as follows.

We inflicted multiple wounds on the leading edge of the lateral epidermis, in an attempt to compromise the integrity of the contractile purse-string throughout the course of dorsal closure. These experiments show that continuity of the purse-string is not required for most or all of the movement of the lateral epidermis during dorsal closure (Fig. 11). Nevertheless, we frequently observed that embryos did not close quite as completely as controls. In such embryos, an irregular scar replaced the neatly zippered epithelial sheets at the dorsal midline (compare wounded embryos in Figs. 6 and 10–12 to the controls shown in Fig. 1 and 3).

Similarly, multiple wounds to the amnioserosa that were designed to compromise the mechanical integrity of this cell sheet also failed to block dorsal closure. This result is most easily seen when the laser was used to target a small cluster of cells towards one end of the amnioserosa. Thus, the spot targeted was essentially equidistant from one end of the amnioserosa and the lateral epidermis (Fig. 12). The data are supported by experiments in which we ablated the entire amnioserosa (not shown). Time-lapsed analysis was initiated and, periodically, the time-lapsed sequence was stopped and a through-focus series was done so that we could evaluate the extent to which healing replaced the cells of the amnioserosa. If there was any indication that the amnioserosa was beginning to heal, the embryo was reirradiated. For this second irradiation and for all subsequent irradiations, approximately four distinct spots on the margins of the initial wound were targeted. In the example shown, the embryo was targeted a total of five times over the course of an hour. By irradiating target cells that were asymmetrically placed in the amnioserosa, we could use the other end of the amnioserosa as a control. Dorsal closure proceeded in the absence of an intact amnioserosa to the point of complete closure.

In some embryos, we also repeatedly wounded both the leading edge of the lateral epidermis and the amnioserosa. Indeed, we even wounded the leading edge on both flanks of the embryo and the amnioserosa in between, creating a cut that extended across the embryo. In each case, extensive damage to the embryo made it difficult to follow the process of dorsal closure. One interpretation is that ablation of both the leading edge and the amnioserosa blocked dorsal closure. An alternative is that the damage was extensive and nonspecific.

Discussion

Time-lapsed video records and laser ablation experiments

allow us to do the following: document cell shape changes during dorsal closure stages in living *Drosophila* embryos; provide evidence for a contractile purse-string at the leading edge of the lateral epidermis; and show that most of the surface of the embryo is under an intrinsic or resting tension. In addition, we use successive ablation studies for the following reasons: to evaluate how specific embryonic structures contribute to dorsal closure; demonstrate that the embryonic epithelium can heal rapidly and extensively; and show that actin is recruited to wound margins and that wounds close in a purse-string–like fashion. These studies provide insight into the nature of forces that contribute to dorsal closure and provide constraints for models that are designed to explain the cellular and molecular mechanisms of dorsal closure. They establish *Drosophila* as a model system for the study of the dynamics of epithelial wounding and wound healing.

The Leading Edge of the Lateral Epidermis Contributes to Dorsal Closure

At the leading edge of the lateral epidermis, an actin-rich contractile band assembles early in dorsal closure and is maintained until the completion of dorsal closure. Concomitant with the recruitment of actin, the shape of the leading edge changes from scalloped and wispy to fairly straight and apparently robust. During the same period, video time-lapsed analyses demonstrate that initially, the leading edge is dynamic, i.e., it advances and retreats locally. Later, the leading edge stabilizes and proceeds to closure in a supracellular purse-string–like fashion. Laser ablation studies confirm that the leading edge is under tension and rapidly snaps apart when cut, similar to a rubber band that is under tension when severed (Fig. 2, a and b, and Figs. 7 and 8). In addition, the progress of the leading edge toward the dorsal midline is transiently inhibited. Together, these studies are consistent with a supracellular, purse-string–like structure that contributes force to dorsal closure.

Purse-string models were initially devised to explain cytokinesis, where a thin contractile ring resides in the cell cortex and is arranged equatorially (for review see Kiehart, 1999). The models hypothesize that tension for ingression of the ring is generated when bipolar myosin filaments tug on antipolar actin filaments that are anchored to the cortex or plasma membrane. Such forces, like the forces generated by a muscle sarcomere, are directed along the straight lines that connect the anchoring points for the actin filaments. Such forces are directed almost, but not quite, tangential to the cell surface. The curvature of the surface allows such forces to be resolved into a vector that is normal to the cell surface. Similarly, the contractility of the individual elements of the supracellular purse-string model is hypothesized to generate forces that are essentially linear and are directed nearly, but not quite, perpendicular to the direction of movement of the leading edge of the lateral epidermis. The curvature of the leading edge allows such forces to be resolved into a net force that is directed dorsally.

The supracellular purse-string at the leading edge, like the intracellular purse-string hypothesized to drive cytokinesis in animal cells, is not strictly comparable to a real purse-string in the conventional sense of a drawstring for closing certain purses. Indeed, the purse-string for dorsal closure is made of a series of contractile elements at the leading edge of each cell. The contractile elements that form the purse-string are as a consequence discontinuous. Mechanical integrity of the cellular or supracellular purse-string as a whole depends on stitching together the individual contractile elements through robust linkages that span the plasma membrane at intercellular junctions. As a consequence, when the dorsal closure purse-string is cut, the structure fails locally, not globally. Cutting a real purse-string would be expected to completely compromise the closure of the mouth of the purse. In laser-irradiated fly embryos, inspection of the tissue adjacent to the site of ablation shows that contraction of the leading edge that results from local relaxation of tension (due to the ablation) appears restricted to ~25–50 μm from the wound edge (Figs. 8 b and 10 f). Thus, the contraction of the leading edge is not distributed throughout the leading edge as would be expected for severing a simple purse-string or a stretched rubber band. As discussed elsewhere (Kiehart, 1999), the intracellular purse-string for cytokinesis also appears to be attached to the cell cortex and/or membrane at high spatial frequency. As a consequence, local disruptions of the cytokinetic purse-string are also spatially restricted (Inoué, 1990). While the overall concept of a cellular or supracellular purse-string is useful and powerful, these structural caveats must be taken into account.

Repeated ablation of the leading edge at one or more sites along its length does not prevent dorsal closure from proceeding to completion. One possibility is that disruption of the contractile purse-string is only transient. Indeed, healing is rapid and the wound purse-string that forms may provide mechanical continuity between the remaining segments of the leading edge purse-string even when the leading edge per se is cut. We consider this possibility unlikely because repeated ablations did not substantially alter the rate at which dorsal closure proceeded compared with the contralateral, nonirradiated side of the embryo (Fig. 11). In addition, the rates of closure for both sides of the experimental embryos were not distinguishably different than the rates of closure of control embryos (which varied considerably).

The region between two ablated segments proceeds dorsally at approximately the same rate as the contralateral side or those segments of the leading edge purse-string that remain anchored to the embryo poles (compare the segment of the purse-string between the wounds in Fig. 11 b to the rest of the purse-string). Again, just after wounding, the leading edge may fail to progress or even lose ground in its march toward the dorsal midline. Nevertheless, these segments appear to recover lost ground and finish dorsal closure even after numerous attempts to disrupt the mechanical integrity of the purse-string (Fig. 11). Recall that our ablation studies indicate that the lateral epidermis is not pushing the leading edge (discussed further below). Moreover, the overall geometry of the small segment of free leading edge that is isolated from the remainder of the leading edge by two wounds is not appropriate for converting tension in the leading edge into forward progress of the leading edge (see above). We conclude that contractility in the amnio-

serosa must be driving the advance of the isolated segments.

Overall, our interpretation is that the leading edge contributes to dorsal closure. In part, the purse-string potentially maintains the integrity and shape of the cells at the leading edge. Recall that, when embryos lack zygotically encoded nonmuscle myosin, the leading edge fails to advance properly and the leading edges of the dorsal-most cells in the advancing lateral epidermis splay considerably (Young et al., 1993). While the leading edge purse-string may facilitate dorsal closure, it is clear that dorsal closure can proceed in the absence of an intact contractile purse-string. We conclude that the defects in myosin may contribute to contractility in other tissues that contribute to dorsal closure.

The Amnioserosa Contributes to Dorsal Closure

Cell shape changes in unperturbed embryos suggest that the amnioserosa itself contracts during dorsal closure. A number of observations suggest that these cell shape changes are due to amnioserosa cell autonomous contractility and that the amnioserosa is not compressed by the advancing, leading edge of the lateral epidermis or other external forces. Our observation that individual cells, completely surrounded by other, amnioserosal cells, can disappear out of the plane of the tissue, suggests that they are actively, and cell autonomously, contractile. We do not understand the mechanism by which the cells move out of the plane of the amnioserosa. One possibility is that the cells simply alter their contacts with their neighbors and crawl out of the plane of the amnioserosa. An alternate hypothesis is that the surrounding cells form a supracellular purse-string that contracts and forces the cell out of the amnioserosa. A likely scenario is that a combination of the two forces is at work. Our observation that ablation of cells in the amnioserosa causes a retreat of the leading edge away from the dorsal midline demonstrates that the amnioserosa is under tension, and that the tension can contribute to the advance of the leading edge. If the amnioserosa was being compressed by the progress of the leading edge or the lateral epidermis, we would expect no change in the position of the leading edge as a consequence of ablation of the amnioserosa. The advance of the small segments of the leading edge that are formed after two ablations suggests further that the amnioserosa contributes to the overall dorsal movement of the leading edge (discussed above). Finally, as dorsal closure proceeds and the leading edge advances toward the dorsal midline, the amnioserosa appears to contract. Thus, cells of the lateral epidermis do not advance over the cells of the amnioserosa.

Together, these observations suggest that contractility of the amnioserosa contributes to dorsal closure. Nevertheless, repeated disruption of this tissue appears to actually speed dorsal closure (the ablated side of the amnioserosa in Fig. 12 finishes closure before the control side). This experiment strongly suggests that the amnioserosa alone cannot be responsible for dorsal closure. Again, while it is possible that the leading edge finds some other tissue to crawl on, we have no evidence for the existence of such a tissue, especially during early stages of dorsal closure (despite repeated, through-focal analysis of the multiply wounded embryos). It is possible that deeper tissues contribute at late stages, but again, we see no direct evidence for such contributions. Moreover, because dorsal closure in unperturbed embryos does not entail a net movement of the lateral epidermis with respect to the edge of the amnioserosa, we suggest that the mechanisms that are usually associated with cell translocation (the extension of actin-rich processes and their subsequent retraction) are not likely to be involved in dorsal closure (for review see Pollard et al., 2000). Our interpretation is that the amnioserosa, like the leading edge, must provide tension that facilitates dorsal closure.

The Lateral Epidermis Produces Forces that Oppose Dorsal Closure

The lateral epidermis provides a key source of increased cellular surface area for dorsal closure. One unlikely possibility is that the lateral epidermis might contribute to pushing the leading edge of the lateral epidermis toward the dorsal midline. Our ablation studies suggest that the lateral epidermis is under tension and retards the forward motion of the leading edge. When sites in the lateral epidermis are ablated, the leading edge abruptly advances toward the dorsal midline (Fig. 9, c–f). As a consequence, we can rule out that dorsal closure is due to forces generated from the active spreading of the lateral epidermis (i.e., pushing).

Multiple Forces Appear To Be Required for the Completion of Dorsal Closure

Our interpretation of the data are that neither the force produced by the contractility of the supracellular purse-string or by the amnioserosa can alone account for the cell sheet movements in dorsal closure because the mechanical integrity of both tissues can be disrupted without blocking dorsal closure. Therefore, we attempted to ablate both the leading edge of the lateral epidermis and the amnioserosa. These experiments were difficult to evaluate because of the extensive damage caused by the multiple irradiations required to ensure that the tissues involved were prevented from healing. Nevertheless, the observation that ablation of both the leading edge of the lateral epidermis and the amnioserosa together appeared to block dorsal closure is intriguing. At this time, the size of the UV microbeam we use for ablation is not diffraction-limited, and is likely too big for studies in which multiple irradiations have to be repeated to disrupt tissue integrity. We are developing methods to deliver a diffraction-limited spot that is variable both in intensity and incident wavelength over a wide range. Such a beam may be more useful for the cycles of wounding that would be required to unambiguously identify the source of the forces for dorsal closure.

A summary of our findings is presented schematically in Fig. 13. Panel a is a sketch of tissues relevant to our studies in an embryo midway through dorsal closure. In b–d, the arrows represent the direction of movements that follow ablation. Forces generated in the leading edge of the lateral epidermis and in the amnioserosa can contribute to the movement of the leading edge of the lateral epidermis toward the dorsal midline. Forces in the flank of the lateral epidermis oppose that movement.

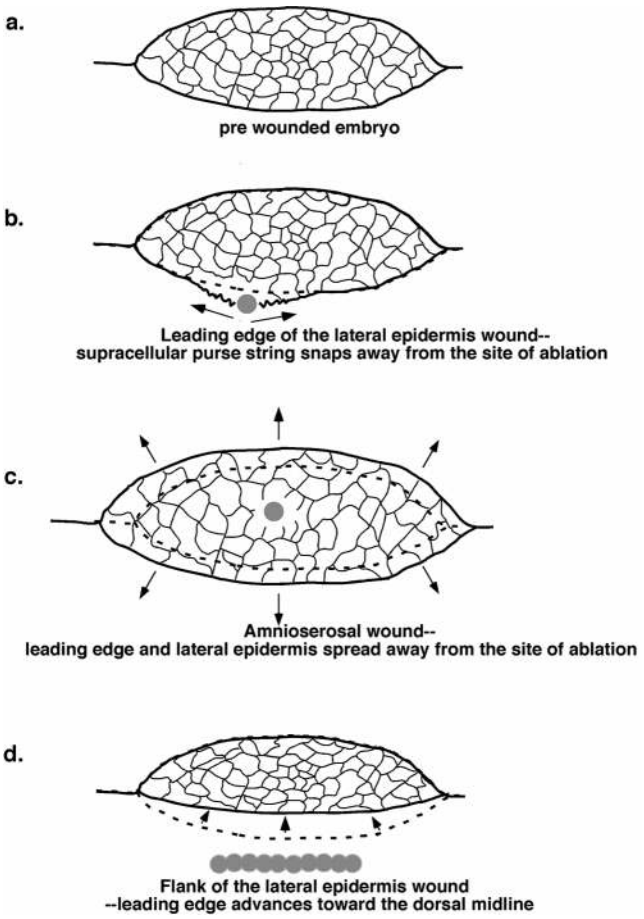

Figure 13. A schematic diagram of dorsal epithelial tissues in a midstage 14 embryo indicates the forces that contribute to cell movement during dorsal closure. (a) Tracing of the shape of the leading edge (LE) of the lateral epidermis and of cell shape in the amnioserosa (AS, traced from images of a wild-type embryo before wounding). b–d show wounds to different epithelial tissues. In each case, the ablating spot is shown as a gray circle, and the outline of the leading edge of the lateral epidermis before wounding is shown as a heavy dotted line (in some cases it superimposes on the outline of the leading edge after wounding). Arrows depict the direction of tissue movement after ablation. (b) A wound to the leading edge of the lateral epidermis causes recoil of the leading edge away from the site of ablation and away from the dorsal midline. (c) A wound to the amnioserosa causes nearly isotropic spreading away from the site of ablation. (d) A series of wounds to the flank of the lateral epidermis releases tension on the leading edge and allows it to advance prematurely towards the dorsal midline.

Intrinsic Tension of Tissues

The mechanical properties of cells and tissues have been investigated previously (e.g., Thompson, 1917; Cooke, 1975; Wainwright, 1988). Our experiments confirm the overall mechanical properties of developing (Beloussov et al., 1997; Van Essen, 1997) and mature tissues (Omens and Fung, 1990), and how such properties might contribute to forces for morphogenesis or tissue homeostasis. Here, we apply a biomechanical analysis to a simple tissue in a genetically tractable organism and establish constraints for models that seek to explain dorsal closure.

The intrinsic tension observed when the leading edge of the lateral epidermis or the amnioserosa relaxes after ablation may be due to forces generated by nonmuscle myosin II. Specifically, our studies on myosin II function in *Drosophila* suggested a purse-string structure that here we demonstrate is contractile. Further, our analysis of myosin II function in oogenesis demonstrated that the migration of a small cluster of follicle cells, called border cells, requires myosin function (Edwards and Kiehart, 1996; for review of border cell migrations see Montell, 1999). At the light microscope level, myosin and actin are appropriately positioned in the border cells to drive traction-mediated migration. At the electron microscope level, actin filaments bundles are seen both parallel and perpendicular to the leading edge of the lateral epidermis during dorsal closure (Rickoll, W.L., and D.P. Kiehart, unpublished observations). Thus, the orientation of these filaments are such that they can contribute both to the contractility of the supracellular purse-string and be responsible for traction-mediated migration of cells in the lateral epidermis. While our data suggest that the actin bundles oriented perpendicular to the leading edge do not mediate net translocation of the lateral epidermis with respect to the amnioserosa, such filaments may, nevertheless, be important for transmitting tension between the amnioserosa and the lateral epidermis.

To understand better the forces involved in both morphogenesis and wound healing, we expect to use the power of classical and modern molecular genetics that are available in the *Drosophila* system. We have already attempted experiments designed to test directly a role for nonmuscle myosin-II in movement of the leading edge of the lateral epidermis during dorsal closure. We wounded embryos that were homozygous for mutations in the *zipper* gene, which encodes the nonmuscle myosin II heavy chain, in a genetic background that included the sGMCA actin/cytoskeleton cell shape marker. In a number of experiments, contractility of the leading edge is compromised: the leading edge of irradiated *zip* homozygotes fails to spring apart like its wild-type counterparts shown in Figs. 6 and 7 (data not shown). These results suggest that myosin is a key component of the contractile supracellular purse-string. Nevertheless, we also observe cases in which the leading edge behaves as in wild-type embryos. Our interpretation is that perdurance of maternal *zipper* product (see Young et al., 1993) complicates interpretation of these experiments. A more definitive analysis of the role of myosin in contractility for dorsal closure will require mosaic analysis that either depletes myosin in local regions of the leading edge (Xu and Rubin, 1993), or supplies myosin to local regions of the leading edge through GAL4/UAS-based expression (Brand et al., 1994) in an otherwise homozygous myosin mutant background.

Drosophila as a Model System for the Study of Wounding and Wound Healing in Epithelia

Rapid healing of the lateral epidermis suggests that this is an excellent model system for the design of genetic strategies to evaluate the molecular basis of wound healing. The wide variety of mutations for components of signaling and structural pathways suggest that analysis of wound healing in the fly will be valuable. As described below, we have al-

ready begun to analyze the contractile and motile properties of the leading edge in flies homozygous for recessive mutation in the *zipper* gene. We are poised to begin studies on the signaling pathways that regulate myosin-II function and have begun to evaluate other pathways that are believed to contribute to wound healing in vertebrates. Of course, the most powerful use of the *Drosophila* system would be analysis of genes whose products contribute to wound healing through forward genetic screens designed to identify loci that are required for wound healing.

We thank the members of the Kiehart lab, Mike Sheetz, Celeste Berg, Rick Fehon, and Robin Wharton for insightful comments made throughout the course of this work. We thank Mark Peifer and members of his lab for additional comments. We thank Ron Sterba for technical assistance in setting up the laser microbeam and image processing and analysis. We thank Clare Jen and Erin Swails for assistance with tracking cell positions. We thank Susan Halsell for critically reading the manuscript and a number of valuable suggestions. Finally, we thank the efforts of two anonymous reviewers whose comments were most insightful.

This study was supported by grants from the National Institutes of Health (GM33830) and Office of Naval Research (N00014-97-1-0911).

Submitted: 15 October 1999
Revised: 10 March 2000
Accepted: 14 March 2000

References

Agnes, F., and S. Noselli. 1999. La fermeture dorsale chez la *Drosophile*. Un modèle génétique del cicatrisation? (Dorsal closure in *Drosophila*. A genetic model for wound healing?). *C.R. Acad. Sci. Paris, Sciences de la vie.* 322:5–13.

Beloussov, L.V., N.I. Kazakova, N.N. Luchinskaia, and V.V. Novoselov. 1997. Studies in developmental cytomechanic. *Intl. J. Dev. Biol.* 41:793–799.

Bement, W.M., P. Forscher, and M.S. Mooseker. 1993. A novel cytoskeletal structure involved in purse string wound closure and cell polarity maintenance. *J. Cell Biol.* 121:565–578.

Bement, W.M., C. Mandato, and M.N. Kirsch. 1999. Wound-induced assembly and closure of an actomyosin purse string in *Xenopus* oocytes. *Curr. Biol.* 9:579–587.

Brand, A.H., A.S. Manoukian, and N. Perrimon. 1994. Ectopic expression in *Drosophila*. *In Drosophila melanogaster*: Practical Uses in Cell and Molecular Biology. L.S.B. Goldstein and E.A. Fyrberg, editors. Academic Press, San Diego, CA. 635–654.

Brock, J., K. Midwinter, J. Lewis, and P. Martin. 1996. Healing of incisional wounds in the embryonic chick wing bud: characterization of the actin purse-string and demonstration of a requirement for Rho activation. *J. Cell Biol.* 135:1097–1107.

Campos-Ortega, J.A., and V. Hartenstein. 1985. The Embryonic Development of *Drosophila melanogaster*. Springer-Verlag, New York. 227 pp.

Campos-Ortega, J.A., and V. Hartenstein. 1997. The Embryonic Development of *Drosophila melanogaster*. Second Edition. Springer-Verlag, New York. 405 pp.

Cooke, J. 1975. Control of somite number during morphogenesis of a vertebrate, *Xenopus laevis*. *Nature*. 254:196–199.

Edwards, K.A., and D.P. Kiehart. 1996. *Drosophila* nonmuscle myosin II has multiple essential roles in imaginal disc and egg chamber morphogenesis. *Development*. 122:1499–1511.

Edwards, K.A., M. Demsky, R.A. Montague, N. Weymouth, and D.P. Kiehart. 1997. GFP-moesin illuminates actin cytoskeleton dynamics in living tissue and demonstrates cell shape changes during morphogenesis in *Drosophila*. *Dev. Biol.* 191:103–117.

Elul, T., M.A. Koehl, and R. Keller. 1997. Cellular mechanism underlying neural convergent extension in *Xenopus laevis* embryos. *Dev. Biol.* 191:243–258.

Greulich, K., and G. Leitz. 1994. Light as microsensor and micromanipulator: laser microbeams and optical tweezers. *Exp. Tech. Phys.* 40:1–14.

Harden, N., M. Ricos, Y.M. Ong, W. Chia, and L. Lim. 1999. Participation of small GTPases in dorsal closure of the *Drosophila* embryo: distinct roles for Rho subfamily proteins in epithelial morphogenesis. *J. Cell Sci.* 112:273–284.

Inoué, S. 1990. Dynamics of mitosis and cleavage. *Ann. NY Acad. Sci.* 582:1–14.

Irvine, K.D., and E. Wieschaus. 1994. Cell intercalation during *Drosophila* germband extension and its regulation by pair-rule segmentation genes. *Development*. 120:827–841.

Jordan, P., and R. Karess. 1997. Myosin light chain-activating phosphorylation sites are required for oogenesis in *Drosophila*. *J. Cell Biol.* 139:1805–1819.

Jurgens, G., E. Wieschaus, C. Nüsslein-Volhard, and H. Kluding. 1984. Mutations affecting the pattern of the larval cuticle in *Drosophila melanogaster* II. Zygotic loci on the third chromosome. *Roux's Arch. Dev. Biol.* 193:283–294.

Karess, R.E., X. Chang, K.A. Edwards, S. Kulkarni, I. Aguilera, and D.P. Kiehart. 1991. The regulatory light chain of nonmuscle myosin is encoded by spaghetti-squash, a gene required for cytokinesis in *Drosophila*. *Cell*. 65: 1177–1189.

Keller, R.E. 1980. The cellular basis of epiboly: an SEM study of deep-cell rearrangement during gastrulation in *Xenopus laevis*. *J. Embryol. Exp. Morphol.* 60:201–234.

Keller, R.E., and J.P. Trinkaus. 1987. Rearrangement of enveloping layer cells without disruption of the epithelial permeability barrier as a factor in Fundulus epiboly. *Dev. Biol.* 120:12–24.

Kiehart, D.P. 1999. Wound healing: the power of the purse string. *Curr. Biol.* 9:R602–R605.

Kiehart, D.P., R.A. Montague, W.L. Rickoll, D. Foard, and G.H. Thomas. 1994. High-resolution Microscopic Methods for the Analysis of Cellular Movements in *Drosophila* Embryos. Academic Press, San Diego. 507–532.

Knust, E. 1997. *Drosophila* morphogenesis: movements behind the edge. *Curr. Biol.* 7:R558–R561.

Leptin, M. 1999. Gastrulation in *Drosophila*: the logic and the cellular mechanisms. *EMBO (Eur. Mol. Biol. Organ.) J.* 18:3187–3192.

Li, Q.J., T.M. Pazdera, and J.S. Minden. 1999. *Drosophila* embryonic pattern repair: how embryos respond to cyclin E-induced ectopic division. *Development*. 126:2299–2307.

Liu, H., Y.C. Su, E. Becker, J. Treisman, and E.Y. Skolnik. 1999. A *Drosophila* TNF-receptor-associated factor (TRAF) binds the ste20 kinase Misshapen and activates Jun kinase. *Curr. Biol.* 9:101–104.

Lu, Y., and J. Settleman. 1999. The *Drosophila* Pkn protein kinase is a Rho/Rac effector target required for dorsal closure during embryogenesis. *Genes Dev.* 13:1168–1180.

Martin, P. 1997. Wound healing-aiming for perfect skin regeneration. *Science*. 276:75–81.

Martin, P., and J. Lewis. 1992. Actin cables and epidermal movement in embryonic wound healing. *Nature*. 360:179–183.

Montell, D.J. 1999. The genetics of cell migration in *Drosophila melanogaster* and *Caenorhabditis* elegans development. *Development*. 126:3035–3046.

Omens, J.H., and Y.C. Fung. 1990. Residual strain in rat left ventricle. *Circ. Res.* 66:37–45.

Pollard, T.D., L. Blanchoin, and R.D. Mullins. 2000. Molecular mechanisms controlling actin filament dynamics in nonmuscle cells. *Annu. Rev. Biophys.* In press.

Ricos, M.G., N. Harden, K.P. Sem, L. Lim, and W. Chia. 1999. Dcdc42 acts in TGF-beta signaling during *Drosophila* morphogenesis: distinct roles for the Drac1/JNK and Dcdc42/TGF-B cascades in cytoskeletal regulation. *J. Cell Sci.* 112:1225–1235.

Rugendorff, A., A. Younossi-Hartenstein, and V. Hartenstein. 1994. Embryonic origin and differentiation of the *Drosophila* heart. *Roux's Arch. Dev. Biol.* 203:266–280.

Sawamoto, K., P. Winge, S. Koyama, Y. Hirota, C. Yamada, S. Miyao, S. Yoshikawa, M.H. Jin, A. Kikuchi, and H. Okano. 1999. The *Drosophila* Ral GTPase regulates developmental cell shape changes through the Jun NH_2-terminal kinase pathway. *J. Cell Biol.* 146:361–372.

Smith, J.L., and G.C. Schoenwolf. 1997. Neurulation: coming to closure. *Trends Neurosci.* 20:510–517.

Thompson, D. 1917. On Growth and Form. Cambridge University Press, Cambridge, UK. 793 pp.

Turner, F.R., and A.P. Mahowald. 1977. Scanning electron microscopy of *Drosophila melanogaster* embryogenesis. II. Gastrulation and segmentation. *Dev. Biol.* 57:403–416.

Turner, F.R., and A.P. Mahowald. 1979. Scanning electron microscopy of *Drosophila melanogaster* embryogenesis. *Dev. Biol.* 68:96–109.

Van Essen, D.C. 1997. A tension-based theory of morphogenesis and compact wiring in the central nervous system. *Nature*. 385:313–318.

Wainwright, S.A. 1988. Axis and Circumerence. The Cylindrical Shape of Plants and Animals. Harvard University Press, Cambridge, MA.

Wheatley, S., S. Kulkarni, and R. Karess. 1995. *Drosophila* nonmuscle myosin II is required for rapid cytoplasmic transport during oogenesis and for axial nuclear migration in early embryos. *Development*. 121:1937–1946.

Wieschaus, E., and C. Nusslein-Volhard. 1986. Looking at embryos. *In Drosophila*: A Practical Approach. D.B. Roberts, editor. IRL Press, Washington, DC. 199–227.

Williams-Masson, E.M., A.N. Malik, and J. Hardin. 1997. An actin-mediated two-step mechanism is required for ventral enclosure of the *C. elegans* hypodermis. *Development*. 124:2889–2901.

Xu, T., and G.M. Rubin. 1993. Analysis of genetic mosaics in developing and adult *Drosophila* tissues. *Development*. 117:1223–1237.

Young, P.E., T.C. Pesacreta, and D.P. Kiehart. 1991. Dynamic changes in the distribution of cytoplasmic myosin during *Drosophila* embryogenesis. *Development*. 111:1–14.

Young, P.E., A.M. Richman, A.S. Ketchum, and D.P. Kiehart. 1993. Morphogenesis in *Drosophila* requires nonmuscle myosin heavy chain function. *Genes Dev.* 7:29–41.

Zecchini, V., K. Brennan, and A. Martinez-Arias. 1999. An activity of Notch regulates JNK signalling and affects dorsal closure in *Drosophila*. *Curr. Biol.* 9:460–469.